Clays and Clay Minerals, Vol. 35, No. 2, 89–110, 1987.

DISTRIBUTION AND CHEMISTRY OF DIAGENETIC MINERALS AT YUCCA MOUNTAIN, NYE COUNTY, NEVADA

D. E. Broxton, D. L. Bish, and R. G. Warren

Earth and Space Sciences Division, Los Alamos National Laboratory
Los Alamos, New Mexico 87545

Abstract—Yucca Mountain is being studied as a potential site in southern Nevada for an underground, high-level nuclear waste repository. A major consideration for selecting this site is the presence of abundant zeolites in Miocene ash-flow tuffs underlying the region. Beneath Yucca Mountain four diagenetic mineral zones have been recognized that become progressively less hydrous with depth.

Zone I, the shallowest zone, is 375–584 m thick in the central part of Yucca Mountain, but 170 m thick to the north. Zone I contains vitric tuffs that consist of unaltered volcanic glass and minor smectite, opal, heulandite, and Ca-rich clinoptilolite. Zone II thins south to north from 700 to 480 m and is characterized by complete replacement of volcanic glass by clinoptilolite with and without mordenite, and by lesser amounts of opal, K-feldspar, quartz, and smectite. Zone III thins south to north from 400 to 98 m thick and consists of analcime, K-feldspar, quartz, and minor calcite and smectite. Heulandite occurs locally at the top of zone III in the eastern part of Yucca Mountain. Zone IV occurs in the deepest structural levels of the volcanic pile and is characterized by albite, K-feldspar, quartz, and minor calcite and smectite.

Clinoptilolite and heulandites in zone I have uniform Ca-rich compositions (60–90 mole % Ca) and Si:Al ratios that are mainly between 4.0 and 4.6. In contrast, clinoptilolites deeper in the volcanic sequence have highly variable compositions that vary vertically and laterally. Deeper clinoptilolites in the eastern part of Yucca Mountain are calcic-potassic and tend to become more calcium-rich with depth. Clinoptilolites at equivalent stratigraphic levels on the western side of Yucca Mountain have sodic-potassic compositions and tend to become more sodium-rich with depth. Despite their differences in exchangeable cation compositions these two deeper compositional suites have similar Si:Al ratios, generally between 4.4 and 5.0. Analcimes have nearly pure end-member compositions, typical of these minerals formed by diagenetic alteration of siliceous volcanic glass; however, K-feldspars are Si-rich compared to the ideal feldspar formula.

Bulk-rock contents of Si, Na, K, Ca, and Mg of zeolitic tuffs generally differ significantly from stratigraphically equivalent vitric tuffs, suggesting that zeolite diagenesis took place in an open chemical system. Both the whole rock and the clinoptilolite are relatively rich in Ca and Mg in the eastern part of Yucca Mountain and rich in Na in the western part. The Ca- and Mg-rich compositions of the zeolitized tuffs in the eastern part of Yucca Mountain may be due to cation exchange by the sorptive minerals with ground water partially derived from underlying Paleozoic carbonate aquifers.

Diagenetic zones become thinner and occur at stratigraphically higher levels from south to north across Yucca Mountain, probably due to a higher geothermal gradient in the northern part of the area. The diagenetic zones were established when the geothermal gradient was greater than it is today, probably during the thermal event associated with the development of the Timber Mountain-Oasis Valley caldera complex north of Yucca Mountain.

Key Words—Analcime, Chemical composition, Clinoptilolite, Diagenesis, Heulandite, Mordenite, Open system, Zeolites.

INTRODUCTION

Yucca Mountain is located along the southwest border of the Nevada Test Site (NTS), Nye County, Nevada (Figure 1). The mountain is being studied by the U.S. Department of Energy (DOE) and its subcontractors as a potential site for an underground, high-level nuclear waste repository. A major consideration for choosing Yucca Mountain as a potential repository is the presence of abundant zeolites in thick Tertiary ash-flow tuffs that underlie the region (Johnstone and Wolfsberg, 1980). These zeolites, most of which formed by diagenetic alteration of vitric tuffs, are highly selective for certain cationic radionuclides and could provide important natural barriers to their migration. One of the goals of the mineralogic and petrologic studies at Yucca Mountain is to determine the distribution and chemistry of diagenetic minerals at Yucca Mountain and understand the factors that controlled their occurrence.

GEOLOGIC SETTING

Geology

Yucca Mountain is in the southwest Nevada volcanic field of the southern Great Basin and is a remnant of a Miocene-Pliocene volcanic plateau that was centered around the Timber Mountain-Oasis Valley caldera complex (Christiansen *et al.*, 1965, 1977; Byers *et al.*, 1976). North–south trending basin-and-range faults have disrupted the volcanic plateau and formed linear mountain ranges separated by sediment-

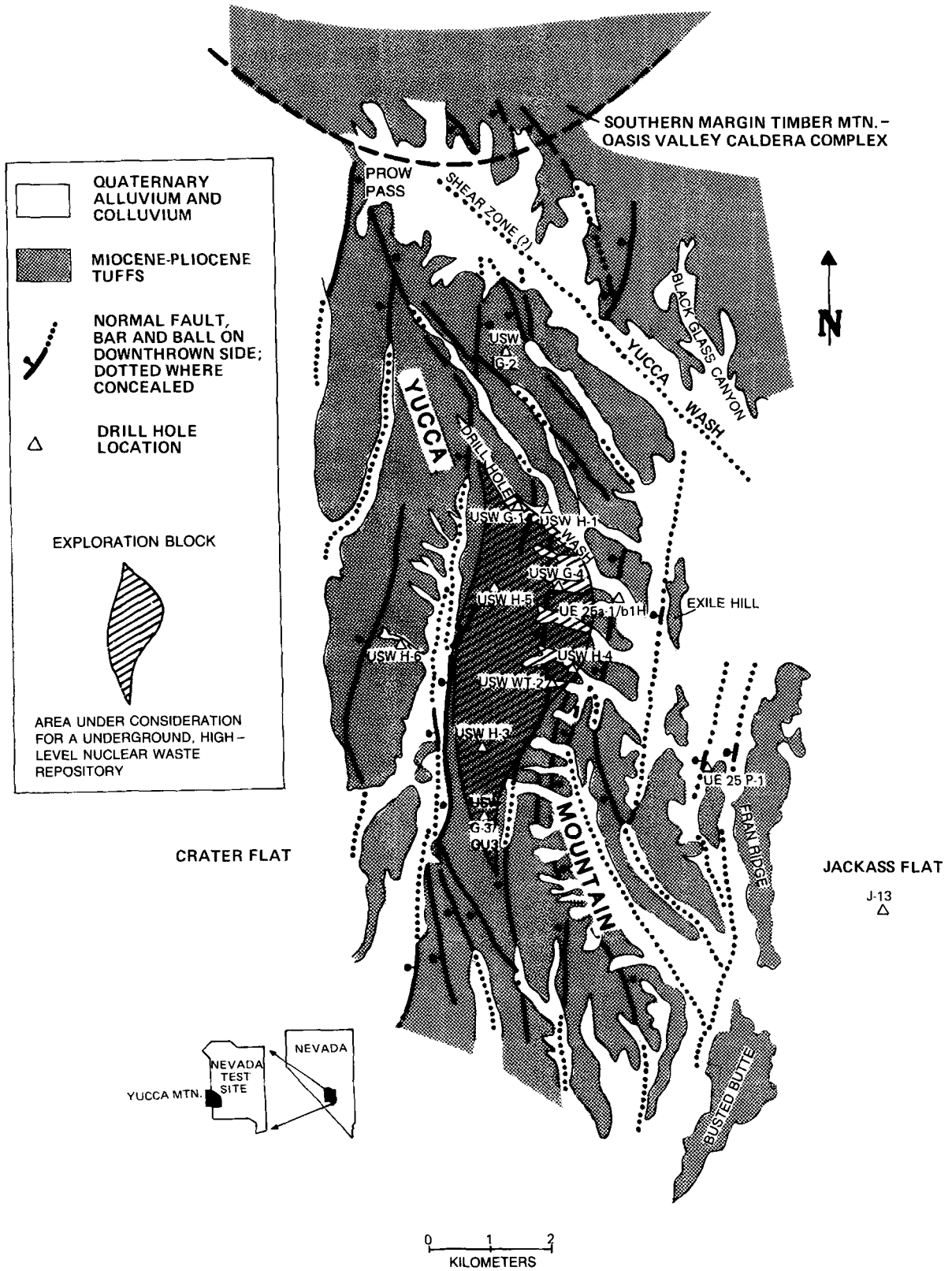

Figure 1. Location map for Yucca Mountain, Nevada.

https://doi.org/10.1346/CCMN.1987.0350202 Published online by Cambridge University Press

Table 1. Stratigraphy of volcanic units at Yucca Mountain, Nevada.[1]

Stratigraphic unit	Thickness (m)	Lithology
Paintbrush Tuff		
Tiva Canyon Member	45–150	Ash-flow tuff; compound cooling unit; nonwelded vitric base; moderately to densely welded, devitrified interior with some vapor-phase crystallization.
Yucca Mountain Member	0–30	Ash-flow tuff; nonwelded vitric top and base; partially welded devitrified interior with some vapor-phase crystallization; present under northern half of Yucca Mountain.
Pah Canyon Member	0–80	Ash-flow tuff; nonwelded and vitric throughout; present under northern half of Yucca Mountain.
Topopah Spring Member	240–365	Ash-flow tuff; compositionally zoned, compound cooling unit; nonwelded zones at top and base and moderately to densely welded, devitrified interior with zones of vapor-phase crystallization; vitrophyres at top and base of unit; zeolites occur both on top of basal vitrophyre and in nonwelded base of unit.
Tuff of Calico Hills	35–290	Ash-flow tuff; nonwelded to partially welded; thoroughly zeolitized at north end of exploration block; becomes vitric southward.
Crater Flat Tuff		
Prow Pass Member	85–190	Ash-flow tuff; nonwelded zones at top and base; moderately welded, devitrified interior with minor vapor-phase crystallization; nonwelded base is zeolitic; nonwelded top zeolitic in northern part of Yucca Mountain, but vitric to the south.
Bullfrog Member	90–190	Ash-flow tuff; compound cooling unit; nonwelded top and base, nonwelded to densely welded interior with thickness and occurrence of welding zones highly variable; zeolitic in nonwelded zones.
Tram Member	155–385	Ash-flow tuff; compound cooling unit; zones of partial to dense welding vary from drill hole to drill hole; zeolitic in its nonwelded to partially welded parts; otherwise devitrified.
Dacite Flow Breccia	0–120	Flow breccia, lava, and tuffs; occurrence restricted to drill hole USW G-1; zeolites irregularly distributed throughout the unit.
Lithic Ridge Tuff	185–305	Ash-flow tuff; nonwelded to moderately welded; devitrified, contains few zeolite horizons.
Unnamed older tuffs and lavas	365+	Ash-flow tuffs, lavas, reworked volcanic sediments; dacitic to rhyolitic compositions; contains few zeolite horizons.

[1] Spengler *et al.* (1979, 1981), Maldonado and Koether (1983), Scott and Castellanos (1984).

filled troughs. Yucca Mountain is an east-tilted fault-block uplift that has been modified by northwest-trending strike-slip faults (Christiansen *et al.*, 1965; Scott and Spengler, 1982; Scott and Bonk, 1984; Carr, 1984).

Ash-flow tuffs are the predominant lithology at Yucca Mountain (Table 1). Most tuffs are high-silica rhyolites, but two large-volume ash-flow cooling units in the upper part of the sequence are compositionally zoned, grading upward from rhyolite to quartz latite (Lipman *et al.*, 1966; Byers *et al.*, 1976). Exposed bedrock at Yucca Mountain consists primarily of these two zoned tuffs, the Topopah Spring Member (13.3 m.y.) and the Tiva Canyon Member (12.7 m.y.) of the Paintbrush Tuff. The Paintbrush Tuff erupted from the Claim Canyon caldera just north of Yucca Mountain (Byers *et al.*, 1976). Beneath the Paintbrush Tuff, the principal stratigraphic units are in descending order: tuff of Calico Hills, Crater Flat Tuff (13.6 m.y.), Tuff of Lithic Ridge, and a thick, unnamed sequence of ash-flow tuffs and intercalated lavas (Spengler *et al.*, 1979, 1981; Maldonado and Koether, 1983; Carr *et al.*, 1984). Wells on Yucca Mountain have penetrated to depths of 1.8 km without leaving volcanic rocks. East of Yucca Mountain, the volcanic section is about 1.2 km thick and overlies the Silurian Lone Mountain Dolomite (Carr *et al.*, 1986).

Lithology

Diagenetic alteration is most highly developed in nonwelded ash-flow tuff, bedded tuff, and in thin envelopes of nonwelded tuff at the top and bottom of cooling units that have densely welded, devitrified interiors. These nonwelded tuffs were vitric after emplacement and were highly susceptible to alteration because of the instability of volcanic glass in the presence of ground water. Where altered, the tuffs form mappable zones of diagenetic minerals that can be correlated laterally across most of the Yucca Mountain.

MATERIALS AND METHODS

Data sources and samples

All X-ray powder diffraction (XRD) analyses and some mineral chemical and petrographic data were compiled from reports by Sykes *et al.* (1979), Heiken and Bevier (1979), Bish *et al.* (1981), Caporuscio *et al.* (1982), Broxton *et al.* (1982), Vaniman *et al.* (1984), Levy (1984a), Bish and Vaniman (1985), and Broxton *et al.* (1986). New petrographic, mineral chemical, and bulk rock chemical data are also presented here. Except for a few samples from outcrops, all mineralogic and chemical analyses were performed on core and, to a lesser extent, cuttings collected from drill holes shown in Figure 1.

Analytical techniques

Petrographic studies of polished thin sections employed both transmitted- and reflected-light microscope techniques. Chemical compositions of volcanic glasses, zeolites, and authigenic feldspars were determined on an automated Cameca electron microprobe operated at 15 keV and a 15–20-nA beam current. Standards used for calibration of major chemical components included a set of natural feldspars, py-

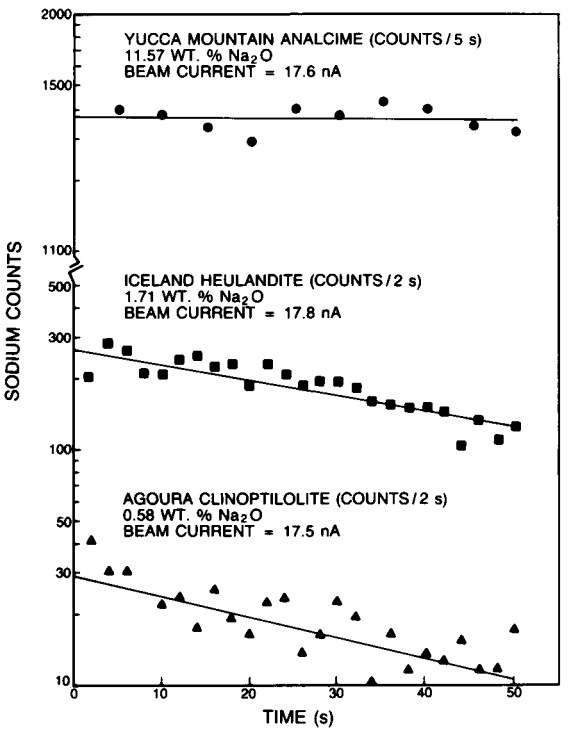

Figure 2. Semi-logarithmic plot showing behavior of Na in zeolites under a stationary electron microprobe beam using an accelerating potential of 15 keV and a rastered beam having an edge of 20 μm.

roxenes, and amphiboles. Wavelength-dispersive X-ray counts for each element were collected for 10–20 s or less, if 10,000 counts were acquired. Compositions were corrected for differential matrix effects using the method of Bence and Albee (1968). Sodium was counted first because it tends to migrate from the region excited by the electron beam (Nielsen and Sigurdsson, 1981). A square raster electron beam with an edge of 15–25 μm was used to minimize Na migration, dehydration, and structural decomposition of zeolites. Despite this precaution, Na loss was a significant problem for the analysis of clinoptilolite (Figure 2). Sodium concentrations measured in clinoptilolite by the electron microprobe were low by as much as 5–12% of the amount present. Moving the sample beneath the electron beam during analysis decreased the Na loss, but clinoptilolite crystals large enough to allow sample movement were rare. Therefore, some analyses were made of monomineralic aggregates of clinoptilolite concentrated in replaced shards and in groundmass vugs. The structural formulae of all zeolites require that $Al + Fe^{3+} = Na + K + 2(Ca + Mg)$. For plotting purposes, clinoptilolite analyses were accepted if the above equation balanced to within 20%. Analcime and authigenic feldspars showed no Na loss under the analytical conditions used in this study.

Major element analyses of bulk-rock samples were made using an automated Rigaku wavelength-dispersive X-ray fluorescence (XRF) spectrometer. Samples were prepared by crushing and homogenizing 15–20 g of sample in a shatterbox. Duplicate 3-g sample splits were heated to 1000°C for 7 hr, and then 1-g splits were fused with 9 g of lithium tetraborate flux. Heating to 1000°C destroys the zeolites and eliminates gross weighing errors introduced by rapid rehydration of zeolites upon cooling. Elemental concentrations were calculated by comparing XRF intensities for the samples to those for standards of known composition. A fundamental parameters program was used for matrix corrections (Criss, 1980). Bulk-rock Na was determined in a separate sample by atomic absorption (AA) spectrophotometry because as much as 20% of the Na present was lost with volatiles during the heating procedure used for the XRF samples.

Splits of 20 bulk-rock samples were analyzed by John Husler of the University of New Mexico and Norman Suhr of Pennsylvania State University to evaluate the accuracy of the XRF analyses. Silica was determined gravimetrically; ferrous iron was determined titrimetrically. All other elements, including total iron, were analyzed by AA (Husler) and d.c. plasma-emission spectrophotometry (Suhr). Comparison of XRF analyses with those determined by AA and emission spectrophotometry showed the XRF analyses to be acceptable. Except for Na (as discussed above), elemental concentrations determined by the three laboratories generally agreed within 5% for major components and 20% for minor components.

Clinoptilolite-heulandite nomenclature

Clinoptilolite and heulandite are closely related, but distinct, zeolite minerals that differ in composition, properties, stability, and genesis (Mumpton, 1960; Mason and Sand, 1960; Boles, 1972). These minerals cannot be easily distinguished in untreated samples on the basis of optical properties, XRD patterns, or compositions; however, alkali-cation rich clinoptilolite can be heated to 700°C before becoming noncrystalline, whereas heulandite becomes noncrystalline at 350°C (Mumpton, 1960). Using this criterion, clinoptilolite was distinguished from heulandite by heating selected samples to 450°C for 8–12 hr, and then determining the sample crystallinity by XRD. The terms clinoptilolite and heulandite are used only for those samples receiving this heating treatment. The term clinoptilolite-group minerals refers to clinoptilolite and heulandite which have not been heated.

RESULTS

Mineralogic results

Based upon mineralogic studies in drill hole USW G-1, Smyth and Caporuscio (1981) and Bish *et al.* (1981) recognized that the diagenetic mineral assemblages at Yucca Mountain are vertically zoned and progressively less hydrous with depth. They recognized four diagenetic zones similar to those described by Iijima (1975, 1978, 1980) for burial diagenesis of volcanic ash beds in thick sedimentary sequences. Figure 3 is a fence diagram showing the distribution of these diagenetic zones beneath Yucca Mountain. These diagenetic zones crosscut the bedding of volcano-stratigraphic units at a low angle. The principal mineralogic characteristics of these zones are summarized in Table 2.

Zone I. Zone I (Figure 3) is characterized by widespread preservation of volcanic glass within vitric tuffs above the water table. The thickness of zone I varies from 375 to 584 m except near Prow Pass at the extreme north end of Yucca Mountain (Figure 1), where zone I is 170 m thick. Alteration in zone I is characterized by incipient or incomplete transformation of glass to smectite and opal and is generally confined to

https://doi.org/10.1346/CCMN.1987.0350202 Published online by Cambridge University Press

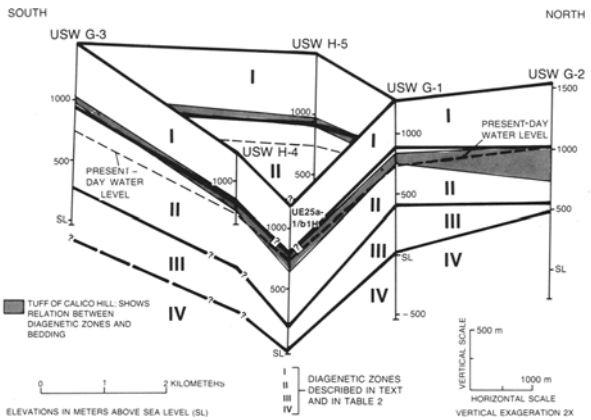

Figure 3. Fence diagram showing distribution of diagenetic zones, Yucca Mountain, Nevada. See Figure 1 for location of drill holes.

fine dust in the groundmass of tuffs. In some samples, smectite forms a coating 3–5 μm thick on the surfaces of partially dissolved shards and pumice vesicles; however, except for hydration, the interiors of these larger pyroclasts are unaltered. Opal occurs as cement in the matrix or as vesicle fillings.

Zeolites occur locally within diagenetic zone I, concentrating in fractures (Arney Carlos, 1985) and in thin discontinuous zones parallel to bedding in mostly vitric tuffs. These local zones of zeolitic alteration generally pinch out laterally; however, an exception occurs near the top of the basal vitrophyre of the Topopah Spring Member where glass is partially altered to smectite and clinoptilolite-group minerals (Levy, 1984a, 1984b). This alteration is most intense within a 0.2–1.0-m-thick zone at the interface between the glassy vitrophyre and overlying densely welded devitrified tuff; smectite commonly makes up 30–50 wt. % of the altered tuff, and clinoptilolite-group minerals, 10–40 wt. %. Alteration of glass to smectites and zeolites also occurs along fractures penetrating the vitrophyre. This zone of alteration occurs in most drill holes and appears to be continuous under much of Yucca Mountain.

Another significant occurrence of zeolites within zone I is found in drill hole USW G-2. Here, 130 m of nonwelded to partially welded ash-flow and bedded tuffs at the base of the Yucca Mountain Member, in the Pah Canyon Member, and at the top of the Topopah Spring Member of Paintbrush Tuff are altered to smectite and clinoptilolite-group minerals. Smectite (30–60 wt. %) is the predominant diagenetic mineral in the upper half of this interval, and smectite (5–50 wt. %) and clinoptilolite-group minerals (10–90 wt. %) are common in the lower half. Unaltered volcanic glass occurs in many of the altered samples, except for the central portion of the Pah Canyon Member which is partially devitrified to a high-temperature mineral assemblage of feldspar and cristobalite. Where present, volcanic glass is generally preserved in larger pyroclasts, such as shards and pumice, whereas the diagenetic minerals replace fine-grain volcanic dust in the tuff matrix. Calcite is present in some of the altered tuffs, commonly filling pumice vesicles of groundmass voids.

Zone II. Zone II (Figure 3) is characterized by nearly complete replacement of volcanic glass by clinoptilolite-group minerals and mordenite. Zone II thins from about 700 to 480 m from south to north and also rises in elevation northward. The top of zone II is about 950 m above sea level in drill hole USW G-3 in the southern part of Yucca Mountain and >1650 m above sea level at the north end of Yucca Mountain, where the zeolitic tuff of Calico Hills crops out at Prow Pass. Between drill holes USW G-3 and USW G-1, the con-

Table 2. Progressive mineral changes with depth in tuffs from Yucca Mountain, Nevada.

Diagenetic zone	Thickness (m)	Characteristic diagenetic mineral assemblages	Remarks
I	170–584	Fresh volcanic glass, smectite, opal, cristobalite	Preservation of glass in vitric tuffs; smectite and opal are the primary alteration minerals. Ca-clinoptilolite and/or heulandite are confined to local zones of alteration. Zone I occurs above the water table.
II	480–700	Clinoptilolite, mordenite, opal, cristobalite, quartz, authigenic K-feldspar, smectite	Original volcanic glass is replaced by clinoptilolite, mordenite, and silica phases. Smectite and authigenic feldspar are minor diagenetic minerals.
III	98–400	Analcime, authigenic K-feldspar, quartz, smectite, calcite	Analcime, quartz, and authigenic K-feldspar replace clinoptilolite, mordenite, opal, and cristobalite. Heulandite is present locally at top of zone III on east side of Yucca Mountain. The cores of some plagioclase phenocrysts are replaced by calcite.
IV	>750	Authigenic albite, authigenic K-feldspar, quartz, smectite, calcite	Authigenic albite replaces analcime. Feldspar phenocrysts locally altered to calcite, authigenic albite, and K-feldspar. Mafic phenocrysts are altered to chlorite, epidote, and iron oxides. Barite, fluorite, and sulfides occur in trace amounts. Diagenetic processes may affect devitrified rocks as well as those rocks that were formally vitric.

https://doi.org/10.1346/CCMN.1987.0350202 Published online by Cambridge University Press

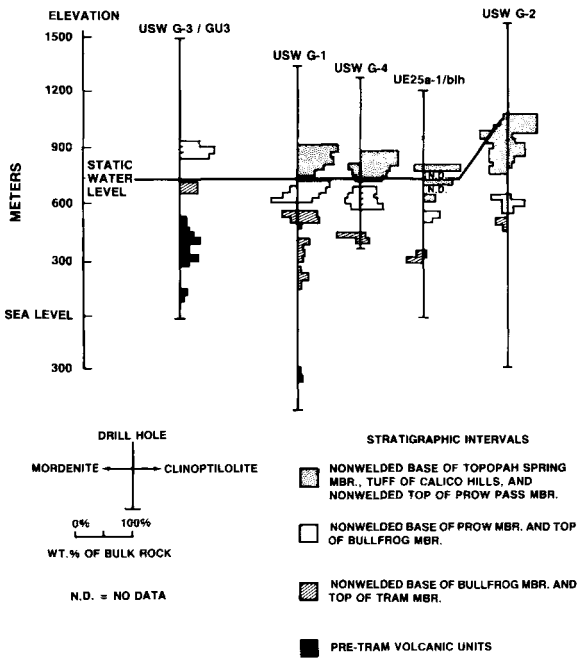

Figure 4. Abundance and distribution of clinoptilolite-group minerals and mordenite, Yucca Mountain, Nevada. Data averaged over 30-m intervals; compiled from Bish and Vaniman (1985) and Bish *et al.* (1981). Stratigraphic units are described in Table 1.

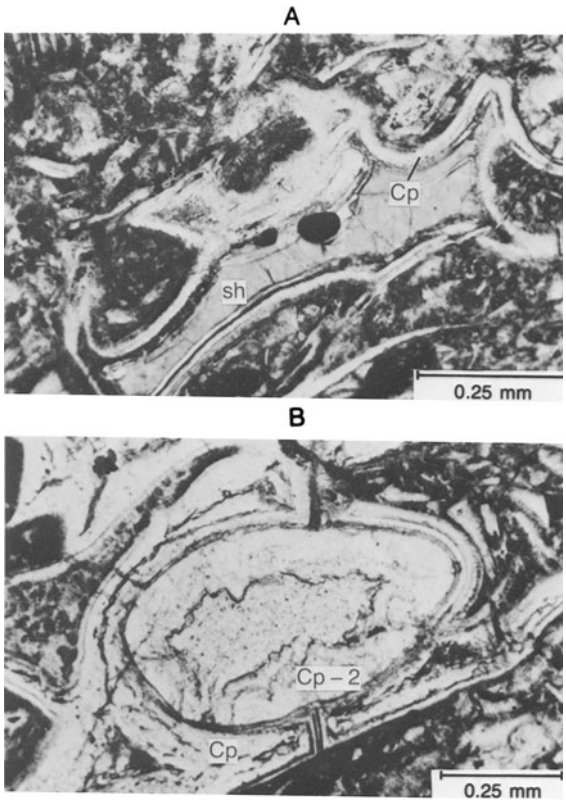

Figure 5. Photomicrographs showing clinoptilolite growth in tuff. A = shard (sh) during early stage of alteration with vitric interior surrounded by inward-encroaching growth rings of clinoptilolite (Cp). B = Advanced stage of alteration with shard framework replaced by clinoptilolite (Cp); other crystals (Cp-2) have grown along vesicle walls and partially filled the open vug.

tact between the zeolitic rocks of zone II and the vitric rocks of zone I is about 225 m above the present-day water table on the west side of Yucca Mountain and 120 m on the east side.

Clinoptilolite-group minerals generally make up 50–75% of the zeolitic tuffs at the top of zone II, but their abundances gradually decrease to 10–20% at the bottom of the zone (Figure 4). Mordenite is an important authigenic phase only in the northern part of Yucca Mountain where it coexists with clinoptilolite-group minerals. The abundance of mordenite is commonly inversely related to that of clinoptilolite-group minerals; mordenite becomes more abundant in the lower part of zone II. Smectite, a common alteration mineral in zone I, makes up <5% of the zeolitic tuffs in diagenetic zone II.

Many vitroclastic textures of the tuffs were preserved during dissolution of volcanic glass and deposition of clinoptilolite-group minerals in resulting cavities (Figure 5). Surface layers of replaced shards and pumices are commonly lined by a 3–5-μm-thick film of smectite. The smectite appears to have grown on the surface of the pyroclast before dissolution or to have precipitated into voids left by retreating glass-dissolution fronts during the earliest stages of glass solution. Interior to the thin smectite layer, layers of 2–10-μm size clinoptilolite-group minerals grew perpendicular to walls of cavities left by retreating glass-dissolution fronts (Figure 5). In more highly altered samples the dissolution of glass in shard interiors is generally more complete. Here, shard centers are commonly empty or partly filled by 10–100-μm size, randomly oriented clinoptilolite-group mineral crystals.

Mordenite occurs as mats of fine, hair-like crystals 10–50 μm long in the open centers of shards. Less commonly, it forms clusters of radiating acicular crystals. Because of mordenite's fine grain size, the chronologic relationship of mordenite to clinoptilolite-group minerals is difficult to determine. The occurrence of mordenite in vugs rimmed by clinoptilolite-group minerals and as hair-like crystals draping clinoptilolite-group minerals suggests that at least some of the mordenite formed later than the clinoptilolite-group minerals. Sheppard and Gude (1985) reported that some mordenite apparently predates and other mordenite postdates clinoptilolite-group minerals at Yucca Mountain.

Other diagenetic minerals in zone II include K-feldspar, opal, and cristobalite. Authigenic K-feldspar oc-

https://doi.org/10.1346/CCMN.1987.0350202 Published online by Cambridge University Press

curs in small amounts in the lower part of zone II. It typically has few nonframework cations other than K (Or_{99-100}) and occurs as 15–30-μm size euhedral crystals that postdate clinoptilolite-group minerals in open vugs. Opal and, more rarely, cristobalite are late stage precipitates, occurring in the centers of vugs rimmed by clinoptilolite. Opal occurs as both isotropic, featureless masses and aggregates of small spheres.

Zone III. Zone III (Figure 3) is characterized by the presence of analcime. The top of zone III has been placed at the first down-hole appearance of analcime, but clinoptilolite-group minerals and mordenite locally persist well below the top of this zone. The thickness of zone III varies from 200 to 400 m throughout most of Yucca Mountain; however, the zone thins to 98 m in drill hole USW G-2 at the northern end of Yucca Mountain.

Analcime occurs both as clusters of euhedral crystals in vugs and as isotropic pseudomorphs of shards and pumice lapilli. These sites of analcime deposition are similar to those of clinoptilolite-group minerals in zone II.

K-feldspar and analcime are intergrown along the margins of vugs. Quartz and calcite occur within vugs lined by analcime and K-feldspar and thus appear to have crystallized later in the diagenetic sequence. Equant crystals of 5–10-μm size quartz occur in the open vugs, whereas calcite forms pseudomorphs of pyroclasts and fills vugs rimmed by analcime and K-feldspar. Calcite appears to be more common on the eastern side of Yucca Mountain compared to the western side. Smectites are minor components of the altered groundmass but seem to be more common in zone III than in the zeolitic tuffs of zone II. The smectites in the northern end of Yucca Mountain are interstratified with progressively more illite with depth in zone III, and ordered illite/smectite occurs toward the bottom of zone III (Bish and Semarge, 1982). Smectites at the southern end of Yucca Mountain, however, show little evidence of the smectite-to-illite transformation (Bish, 1986). The calcic cores of plagioclase phenocrysts in zone III show only slight alteration to calcite and sericite.

Zone IV. Diagenetic zone IV (Figure 3) is characterized by the presence of authigenic albite. The transition from zone III to zone IV is gradational, and the boundary is placed at the first down-hole appearance of albite. The top of zone IV occurs at about the same elevation throughout the Yucca Mountain area, except in drill hole USW G-2 where it is 500 m higher.

Albite first appears as 5–20-μm size euhedral laths that rim and penetrate shards replaced by analcime pseudomorphs. Albite also occurs with K-feldspar and quartz in vugs. Many of the original vitroclastic textures that are obvious in zones I, II, and III have not been observed in zone IV.

Table 3. Representative electron microprobe analyses (wt. %) of volcanic glass, Yucca Mountain, Nevada.

Rock Unit	Pah Canyon Member, perlitic pumice	Topopah Spring Member, perlite in vitrophyre	Tuff of Calico Hills, glass shard	Prow Pass Member, pumice
Sample	G2-547	G3-1227	G3-1537	25a1-2113
SiO_2	73.0	73.9	73.9	75.1
TiO_2	0.09	0.07	0.05	0.00
Al_2O_3	11.9	11.7	11.9	11.4
Fe_2O_3[1]	0.73	0.63	0.64	0.29
MgO	0.00	0.01	0.00	0.00
CaO	0.54	0.36	0.57	0.87
BaO	0.00	0.06	0.15	0.00
Na_2O	3.36	3.33	3.17	3.11
K_2O	4.84	5.55	5.05	4.59
Total	94.5	95.7	95.5	95.4
Si	72.3	72.3	72.6	73.9
Ti	0.06	0.04	0.04	0.00
Al	13.9	13.5	13.8	13.2
Fe^{3+}	0.54	0.45	0.48	0.22
Mg	0.00	0.00	0.00	0.00
Ca	0.56	0.39	0.61	0.92
Ba	0.00	0.02	0.06	0.00
Na	6.46	6.33	6.03	5.94
K	6.11	6.93	6.33	5.77
	Ratio of K, Na, and Ca + Mg			
K	47	51	49	46
Na	49	46	46	47
Ca + Mg	4	3	5	7

[1] Total iron calculated as Fe_2O_3.

The groundmass of zone IV is largely a mixture of cryptocrystalline quartz and feldspar. Calcite and chlorite are minor but ubiquitous authigenic phases that occur as scattered stringers in the groundmass and as shapeless masses that fill open vugs. Plagioclase phenocrysts are completely altered to albite, calcite, and illite in some samples, but are unaltered in other samples. Sanidine phenocrysts are generally less altered than plagioclase, but where altered, they are commonly replaced by authigenic K-feldspar having nearly pure end-member compositions (Or_{100}).

Chemical results

Volcanic glass. Compositions of typical glass shard and pumice samples from several stratigraphic units are listed in Table 3. These volcanic glasses are high-silica rhyolites that contain 3.1–3.4 wt. % Na_2O, 4.5–5.5 wt. % K_2O, and 0.3–0.9 wt. % CaO. $Si/(Al + Fe^{3+})$ ratios range between 4.8 and 5.6. Most glasses are hydrated, typically containing 4–7 wt. % H_2O.

Clinoptilolite-group minerals. Clinoptilolite-group minerals in zone I have similar chemical compositions; they have Si/Al ratios of 4.0–5.0 (Figure 6), and Ca makes up 60–90% of nonframework cations (Table 4; Figure 7). Their Mg contents range from 0.6 to 1.5% MgO. Using the thermal stability criteria of Mumpton (1960), Levy (1984a) determined that some of the Ca-

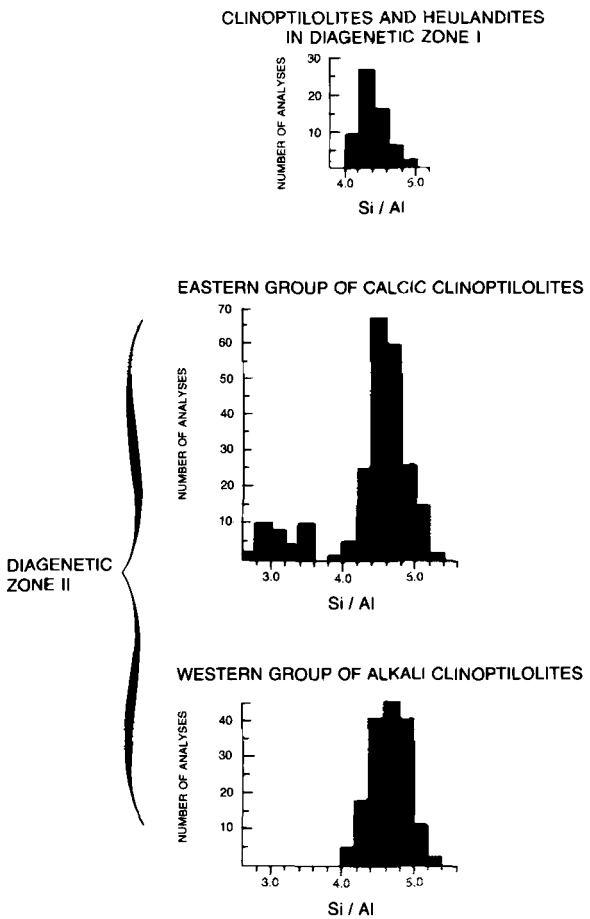

Figure 6. Histograms comparing distribution of Si/Al ratios for clinoptilolite-group minerals from Yucca Mountain, Nevada.

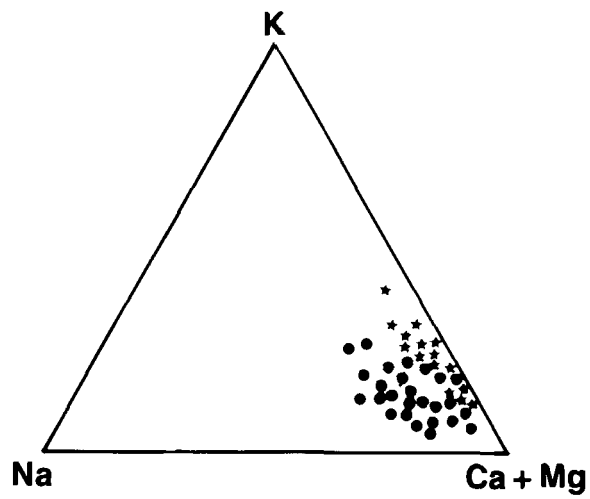

Figure 7. Triangular diagram showing ratios of exchangeable cations in Ca-clinoptilolite and heulandite from diagenetic zone I, Yucca Mountain, Nevada. Compositions of clinoptilolite-group minerals in the Pah Canyon Member in drill hole USW G-2 are shown by the stars; those for the Topopah Spring basal vitrophyre, in drill holes throughout Yucca Mountain, are shown by the solid circles.

rich clinoptilolite-group minerals at the top of the Topopah Spring vitrophyre in zone I appear to be heulandite. Other Ca-rich members of this group at the top of the Topopah Spring vitrophyre, particularly those in drill hole USW G-2, are similar to group-2 clinoptilolites, which have thermal properties intermediate between those of true heulandite and clinoptilolite (Boles, 1972). Heating experiments on Ca-rich clinoptilolites of the Pah Canyon Member in drill hole USW G-2 show that they are also similar to the group-2 clinoptilolites.

Clinoptilolite-group zeolites from diagenetic zone II show more chemical diversity than those from zone I (Table 4). In zone II, the clinoptilolite-group compositions can be subdivided into an "eastern" calcic suite and a "western" alkalic suite, based upon their exchangeable cation contents (Figure 8). A transitional zone in drill holes USW G-4 and USW H-4 contains samples having compositions similar to both suites. The clinoptilolite-group minerals of the eastern calcic suite become more Ca-rich with depth (Figure 8), whereas those of the western alkalic suite become more Na-rich with depth. Both suites are relatively rich in K in the upper part of zone II. The Si/Al ratios for both suites are similar, falling mostly between 4.2 and 5.2 and clustering around 4.6 (Figure 6). The Si/Al ratios for the eastern suite of clinoptilolite-group minerals, however, have a bimodal distribution with a small population of ratios ranging from 2.8 to 3.6. These lower Si/Al ratios occur in the most Ca-rich clinoptilolite-group minerals (Ca > 70% of exchangeable cations) in the deepest parts of zone II and in the upper part of zone III; these clinoptilolite-group minerals are probably heulandites, but they have not been heat-treated to confirm this.

Compared to volcanic glass compositions, clinoptilolite-group minerals are enriched in Ca and Mg, and depleted in Si, Na, K, and Fe (Tables 3 and 4). These chemical differences between clinoptilolite-group minerals and volcanic glass are greatest for calcium-rich zeolites in the eastern part of Yucca Mountain and for zeolites in diagenetic zone I.

Mordenite. Individual mordenite crystals in Yucca Mountain tuffs are so fine-grained and intergrown with other authigenic phases that analysis by electron microprobe and mineral separation techniques were not feasible. Determination of mordenite compositions by bulk-rock techniques was also difficult because monomineralic beds of mordenite are extremely rare at Yucca Mountain. In drill hole USW G-4, two bulk-rock samples containing more than 70% mordenite contain 2.7–2.8% Na_2O, 1.6–2.4% K_2O, and 2.6–2.9% CaO (Broxton *et al.*, 1986, Appendix A, samples 31 and 32).

https://doi.org/10.1346/CCMN.1987.0350202 Published online by Cambridge University Press

Table 4. Representative electron microprobe analyses (wt. %) of clinoptilolite, Yucca Mountain, Nevada.

	Diagenetic zone I		Diagenetic zones II and III								
			Calcic suite, eastern Yucca Mountain				Alkalic suite, western Yucca Mountain				
Rock unit	Pah Canyon Member	Topopah Spring Member	Tuff of Calico Hills	Prow Pass Member	Bullfrog Member	Tuff of Lithic Ridge	Tuff of Calico Hills	Prow Pass Member	Bullfrog Member	Tram Member	Tuff of Lithic Ridge
Sample No.[1]	G2-584	H5-1666	25p1-1250	25p1-1700	25a1-2879	25p1-3330	G1-1774	G3-1874	G3-2615	G3-3589	G3-4423
SiO_2	65.5	65.5	68.6	67.1	56.1	60.6	68.1	68.2	63.9	65.1	65.3
TiO_2	0.00	0.02	0.00	0.00	0.00	0.00	0.00	0.00	0.00	0.00	0.00
Al_2O_3	13.8	13.3	12.4	12.9	16.9	16.0	12.2	11.9	11.7	11.4	12.6
Fe_2O_3[2]	0.00	0.00	0.00	0.00	0.05	0.00	0.00	0.00	0.00	0.51	0.12
MgO	1.47	0.86	0.07	0.32	0.22	0.08	0.09	0.00	0.00	0.12	0.22
CaO	4.23	5.19	3.59	4.37	6.77	7.22	1.11	1.95	1.57	0.79	2.35
BaO	0.02	0.00	0.00	0.05	0.21	0.19	0.03	0.00	0.00	0.19	0.27
Na_2O	0.18	0.17	1.13	1.55	0.89	0.85	2.84	1.69	2.88	2.23	3.21
K_2O	1.09	0.21	3.01	1.23	1.43	0.41	4.20	5.20	2.71	5.55	1.15
Total	86.3	85.2	88.8	87.5	82.6	85.4	88.5	88.9	82.8	85.9	85.2
			Unit-cell composition based on 72 oxygens								
Si	28.9	29.2	29.7	29.4	26.7	27.5	29.8	29.8	29.7	29.7	29.4
Ti	0.00	0.01	0.00	0.00	0.00	0.00	0.00	0.00	0.00	0.00	0.00
Al	7.17	6.98	6.35	6.67	9.44	8.59	6.28	6.14	6.43	6.12	6.70
Fe^{3+}	0.00	0.00	0.00	0.00	0.02	0.00	0.00	0.00	0.00	0.17	0.04
Mg	0.97	0.57	0.04	0.21	0.16	0.05	0.06	0.00	0.00	0.08	0.15
Ca	2.00	2.48	1.67	2.05	3.44	3.51	0.52	0.91	0.78	0.39	1.13
Ba	0.00	0.00	0.00	0.01	0.04	0.03	0.01	0.00	0.00	0.03	0.05
Na	0.15	0.15	0.95	1.32	0.82	0.75	2.41	1.43	2.60	1.97	2.80
K	0.61	0.12	1.66	0.69	0.87	0.24	2.35	2.90	1.61	3.23	0.66
			(Al + Fe)/(2Mg + 2Ca + 2Ba + Na + K)								
	1.07	1.10	1.05	1.02	1.05	1.05	1.06	1.00	1.11	0.99	1.09
			Si/(Al + Fe)								
	4.03	4.18	4.68	4.41	2.82	3.20	4.75	4.85	4.62	4.72	4.36
			Mole % exchangeable cations								
K	16	4	38	16	16	5	44	54	32	57	14
Na	4	4	22	31	15	17	45	27	52	35	59
Ca + Mg	80	92	40	53	69	78	11	19	16	8	27

[1] Sample H5-1666 from Levy (1984a); samples G3-2615, G3-3589, and G3-4423 from Vaniman *et al.* (1984).
[2] Total iron calculated as Fe_2O_3.

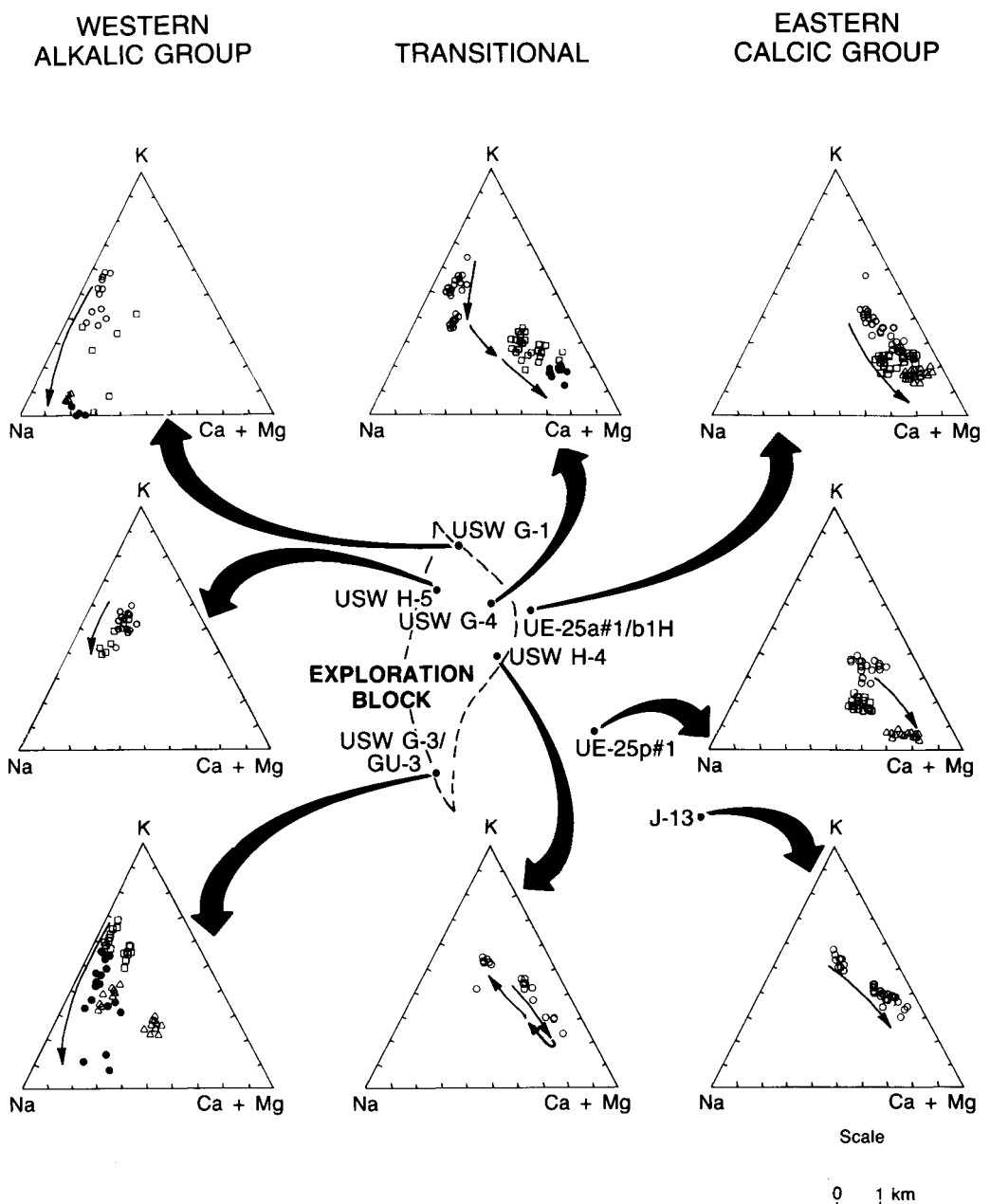

Figure 8. Triangular diagrams showing ratios of exchangeable cations in clinoptilolite-group minerals from diagenetic zones II and III, Yucca Mountain, Nevada.

https://doi.org/10.1346/CCMN.1987.0350202 Published online by Cambridge University Press

Table 5. Representative electron microprobe analyses (wt. %) of analcime, Yucca Mountain, Nevada.

Sample	B1H-3506	25P1-2220	B1H-3393
SiO_2	58.5	59.9	61.9
TiO_2	0.00	0.00	0.00
Al_2O_3	20.6	19.2	18.2
Fe_2O_3	0.0	0.00	0.00
MgO	0.0	0.00	0.00
CaO	0.03	0.00	0.00
BaO	0.00	0.03	0.04
Na_2O	12.7	12.0	11.2
K_2O	0.00	0.00	0.00
H_2O[1]	8.2	8.9	8.7
Total	100.0	100.0	100.0
Unit-cell composition based on 96 oxygens			
Si	33.9	34.8	35.6
Al	14.1	13.1	12.3
Ca	0.02	0.00	0.0
Ba	0.00	0.00	0.01
Na	14.3	13.5	11.7
Si/Al	2.40	2.66	2.89

[1] Water calculated by difference.

These mordenites appear to be slightly more sodic and less calcic than coexisting clinoptilolites.

Analcime. Analcimes from Yucca Mountain show a compositional range from $(NaAl)_{14.3}Si_{33.7}O_{96}\cdot nH_2O$ to $(NaAl)_{12.3}Si_{35.6}O_{96}\cdot nH_2O$. All analcimes analyzed have nearly pure end-member compositions. Analyses of typical analcime crystals by electron microprobe are given in Table 5. Si/Al ratios of analcimes from Yucca Mountain are similar to those from other siliceous volcanic and volcaniclastic rocks (Coombs and Whetten, 1967; Sheppard and Gude, 1973). The 82 analcimes analyzed have Si/Al ratios which range from 2.3 to 2.9 (Figure 9). The distribution of Si/Al ratios appears to be either positively skewed or bimodal, with most of the ratios ranging between 2.5 and 2.6, and a secondary mode occurring between 2.7 and 2.8. Sheppard and Gude (1969) and Boles (1971) showed that the Si/Al ratio in analcime is a function of the silica content of precursor zeolites in some altered tuffs. At Yucca Mountain, however, no relationship between the silica contents of analcimes and those of the two suites of clinoptilolite-group compositions is apparent. The significance of the possible bimodal distribution of Si/Al ratios in analcimes of Yucca Mountain is unknown.

Authigenic feldspars. Authigenic K-feldspar and albite from Yucca Mountain are characterized by nearly pure K and Na compositions, respectively (Table 6). These compositions are typical of feldspars formed under diagenetic conditions (Kastner and Siever, 1979).

The authigenic K-feldspars are somewhat unusual in that, on an 8-oxygen basis, these feldspars contain 0.88–0.96 non-tetrahedral cations rather than the ideal formula of 1.0 cation (Figure 10). The overall charge

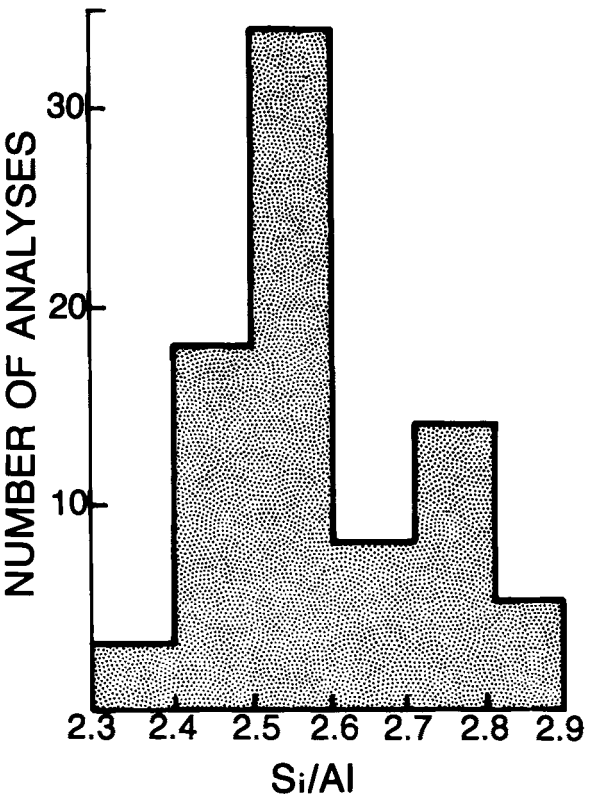

Figure 9. Histogram showing distribution of Si/Al ratios for analcime, Yucca Mountain, Nevada.

of the mineral structure remains balanced because the tetrahedral framework is Si-rich. Si/Al ratios are 3.35–3.45 compared to ideal values of ≤3.00. Several K-feldspar grains were examined by scanning electron microscopy for evidence of intergrown quartz, which could account for their silica-rich nature. X-ray dot maps of K and Si, as well as backscattered electron and X-ray imaging at 2000×, showed no evidence for a separate silica phase in any of the grains examined. Na-loss from these minerals during electron microprobe analysis is not likely, because Na-loss does not occur in sanidine standards or in sanidine phenocrysts analyzed under the same conditions.

Whole-rock chemistry. The chemical compositions of typical Yucca Mountain tuffs are given in Table 7. For comparison, diagenetically altered tuffs are paired with vitric tuffs or with high-temperature, devitrified tuffs from the same stratigraphic horizon; these vitric and devitrified tuffs are assumed to represent original tuff compositions before diagenesis. The composition of vitric tuffs (on a water-free basis) may deviate slightly from the original magmatic compositions because of alkali and alkaline-earth exchange between the tuffs and ground water during hydration (Lipman, 1965; Noble, 1967). Microprobe analyses of individual glass

https://doi.org/10.1346/CCMN.1987.0350202 Published online by Cambridge University Press

Table 6. Representative electron microprobe analyses (wt. %) of authigenic feldspar, Yucca Mountain, Nevada.

	Authigenic K-feldspar		Authigenic albite	
Sample	3-15-82-1	G2-2430	G1-4341	G2-5895
SiO_2	67.9	67.8	67.8	66.7
TiO_2	0.00	0.01	0.02	0.00
Al_2O_3	17.2	16.8	19.6	19.6
FeO	0.00	0.03	0.00	0.00
MgO	0.00	0.00	0.01	0.00
CaO	0.00	0.00	0.16	0.50
BaO	0.00	0.00	0.00	0.03
Na_2O	0.23	0.03	11.8	11.4
K_2O	15.2	15.5	0.01	0.04
Total	100.5	100.2	99.4	98.3
Unit-cell composition based on 8 oxygens				
Si	3.085	3.096	2.981	2.971
Ti	0.000	0.000	0.001	0.000
Al	0.919	0.902	1.016	1.027
Fe^{2+}	0.000	0.001	0.000	0.000
Mg	0.000	0.000	0.001	0.000
Ca	0.000	0.000	0.008	0.024
Ba	0.000	0.000	0.000	0.001
Na	0.020	0.003	1.006	0.984
K	0.881	0.903	0.001	0.002
Σ Tetrahedral cations	4.005	3.999	3.998	3.998
Σ Octahedral cations	0.902	0.906	1.015	1.011
Mole % K, Na, Ca				
K	97.8	99.7	0.1	0.2
Na	2.2	0.3	99.1	97.4
Ca	0.0	0.0	0.8	2.4
Al/(2Fe + 2Mg + 2Ca + 2Ba + Na + K)				
	1.02	1.00	0.99	0.99

shards and pumice lapilli in these vitric tuffs (Table 3) suggest little ion exchange of alkalis or alkaline earths by the glassy pyroclasts; hence, chemical alteration during hydration of vitric tuffs was apparently confined chiefly to the interstitial submicroscopic glass in the matrix. Bulk-rock compositions also differ because phenocrysts and lithic fragments are included in the bulk-rock analyses, but not in the glass analyses.

The compositions of altered tuffs deviate significantly from the original tuff compositions throughout Yucca Mountain, chiefly in alkali and alkaline-earth contents (Table 7). Na and K are generally depleted, whereas Ca and Mg are generally strongly enriched. Fe and Ti show smaller and more variable compositional differences. Si is systematically depleted in the zeolitic tuffs. This depletion of Si is most pronounced for calcic zeolitic tuffs in zones I and II.

A triangular plot of alkalis and alkaline earths (Figure 11) shows a systematic lateral variation across Yucca Mountain. Zeolitic tuff compositions in zone II form two populations (Figure 11A) that closely correspond to the eastern calcic and western alkalic suites of clinoptilolite-group minerals (Figure 8). The compositions of zeolitic tuffs from the western part of zone II overlap original tuff compositions to some extent, but most samples are enriched in Na and depleted in K. Bulk-rock compositions of tuffs from the eastern part of Yucca Mountain deviate most from original tuff compositions, being relatively enriched in Ca and Mg and depleted in Na and K. The bulk-rock compositions of analcime-bearing tuffs in zone III and authigenic albite-bearing tuffs in zone IV also vary laterally across Yucca Mountain (Figure 11B). Tuffs within zones III and IV in the western part of Yucca Mountain tend to be slightly more Na-rich and Ca-poor compared to those in the eastern part. Thus, the chemical dichotomy noted for bulk-rock compositions of zone II also occurs in the deeper diagenetic zones.

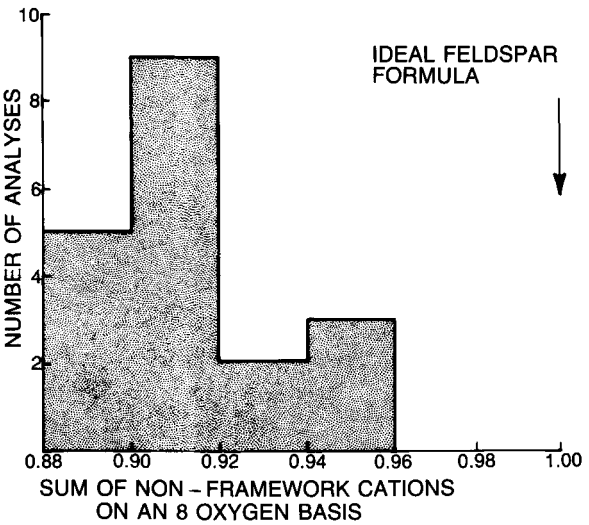

Figure 10. Histogram showing distribution of cations in non-tetrahedral sites of authigenic K-feldspar, Yucca Mountain, Nevada.

DISCUSSION

Open vs. closed system diagenesis

Previous workers have presented conflicting ideas about whether zeolites and their associated diagenetic minerals at the NTS formed in an open or a closed chemical system. Based upon vertical mineralogic and chemical zonations of zeolitic tuffs from the northern and central part of the NTS, Hoover (1968) concluded that zeolitization occurred in an open chemical system, resulting in major mobilization and rearrangement of alkalis and alkaline earths. Moncure *et al.* (1981) found no change in the chemical composition of zeolitic tuffs with depth in drill cores from Pahute Mesa, located in the northwest part of the NTS, and concluded that zeolite diagenesis occurred in a closed chemical system.

To evaluate chemical changes during diagenesis at Yucca Mountain, the compositions of zeolitic rocks in zones I and II were compared with those of stratigraph-

https://doi.org/10.1346/CCMN.1987.0350202 Published online by Cambridge University Press

ically equivalent, unaltered tuffs; samples were compared by normalizing their compositions to the same Al content (Figure 12). Hay (1963) used this method to evaluate chemical changes during the diagenesis of the John Day Formation, reasoning that Al is relatively insoluble and does not migrate significantly during zeolitization. The very low Al content in ground waters from volcanic rocks of the arid southwest suggests that this assumption is reasonable (Lipman, 1965). Figure 12 shows the logarithmic ratio of major elements in zeolitic tuffs to those in unaltered tuffs, normalized to the same Al content. Positive and negative deviations of these ratios from unity indicate net gains or losses, respectively, of chemical constituents from the tuffs during zeolitization.

The data in Figure 12 suggest that Si, Na, K, Ca, and Mg were mobilized to varying degrees during diagenesis (Table 7). Of these, the alkalis and alkaline earths were most strongly affected by zeolitization. Chemical mobility was apparently greatest in the eastern part of Yucca Mountain where the compositions of zeolitic tuffs deviate the most from unaltered tuff compositions (Figures 11A and 12). The variable compositions of zeolitic tuffs suggest that the formation of zeolites from volcanic glass in zones I and II occurred in an open chemical system at Yucca Mountain.

The progressive disappearance of clinoptilolite-group minerals and mordenite and the concurrent increase in analcime with depth indicates that analcime grew at the expense of precursor clinoptilolite and mordenite in zone III. R. A. Sheppard (U.S. Geological Survey, Denver, Colorado, written communication, 1985) reported that analcime has replaced clinoptilolite in the Tram Member in drill hole USW G-1, and that analcime forms pseudomorphs of clinoptilolite in the Prow Pass Member in drill hole USW G-2. Other field studies (Hay, 1966; Sheppard and Gude, 1969) and experimental studies (Boles, 1971; Wirsching, 1976; Höller and Wirsching, 1978; Kirov *et al.*, 1979) have shown that analcime commonly replaces precursor zeolites and does not directly replace volcanic glass.

The bulk-rock chemistry of tuffs in zones III and IV is similar to that of tuffs in zone II despite replacement of clinoptilolite, heulandite, and mordenite by analcime, K-feldspar, and albite (Figure 11). Like the overlying tuffs in zone II, zone III and IV tuffs are subdivided into an eastern calcic suite and a western alkalic suite. Analcime generally constitutes 10–40% of zeolitic tuffs in zone III, whereas clinoptilolite-group minerals commonly constitute 50–75% of zeolitic tuffs in zone II. The amount of analcime formed in zone III was probably limited by the amount of Na freed from precursor clinoptilolite-group minerals. Excess Ca and Mg released by the destruction of clinoptilolite-group minerals was incorporated into calcite and smectite. Excess Si and K probably resulted in the formation of additional K-feldspar, smectite, and quartz. In zone IV, the replacement of analcime by authigenic albite did not significantly change the alkali and alkaline-earth contents of the altered tuffs (Figure 12B).

The mobility of chemical constituents in zone II during zeolitization was probably facilitated by a high permeability within the original nonwelded vitric tuffs. Permeabilities for typical nonwelded vitric tuffs of the NTS range from 2.9×10^{-3} to 7.3×10^{-1} md (Winograd and Thordarson, 1975). During the early stages of diagenesis, cations released to solution by the decomposition of volcanic glass were apparently able to move freely through the tuff before crystallizing within newly forming clinoptilolite-group minerals or before exchanging with pre-existing clinoptilolite-group minerals. As diagenesis progressed, however, the tuffs became increasingly less permeable and movement of pore waters was greatly restricted. Thoroughly zeolitized tuffs of the NTS have permeabilities of about 2.0×10^{-4} md and are usually aquitards (Winograd and Thordarson, 1975). Low permeabilities in these altered tuffs would tend to restrict the transport of soluble cations by ground waters during the mineralogic transformations from zone II to zones III and IV.

Timing of zeolitization

Between drill holes USW G-1 and USW G-3, the boundary between vitric tuffs of zone I and zeolitic tuffs of zone II is a planar surface that dips gently eastward (Figure 3). This surface cuts across stratigraphic contacts of volcanic units which also dip eastward but at a slightly greater angle. These relationships suggest that zeolitization ended before uplift and rotation were completed. Tilting of the stratigraphic units at Yucca Mountain is constrained by the eruptions of the Tiva Canyon Member of Paintbrush Tuff and the Rainier Mesa Member of Timber Mountain Tuff between 11.3 and 12.5 m.y. ago (Scott and Spengler, 1982). The Tuff of Lithic Ridge is one of the oldest volcanic units affected by diagenetic alteration and has a stratigraphically constrained age between units dated at 13.7 and 13.9 m.y. (Carr *et al.*, 1984). Thus, most of the zeolitic deposits at Yucca Mountain formed between 11.3 and 13.9 m.y. ago and were largely contemporaneous with the most active period of silicic volcanism within the southwest Nevada volcanic field.

Little information is available on the time of formation of zones III and IV. The older tuffs probably first acquired the clinoptilolite-group mineralogy of zone II soon after emplacement. Because the older ash flows were progressively buried by younger tuff, however, and because the geothermal gradient probably increased with the intensity of volcanic activity, the less-hydrous mineral assemblage typical of zone III began to replace the clinoptilolite assemblage in the lower parts of the volcanic sequence. Moreover, because zone

Table 7. Representative bulk-rock compositions for tuffs at Yucca Mountain, Nevada.[1]

	Pah Canyon Member, Paintbrush Tuff		Topopah Spring Member, Paintbrush Tuff		Tuff of Calico Hills		
	1A Densely welded devitrified tuff	1B Partially welded, clay- and zeolite-rich tuff	2A Unaltered lower vitrophyre	2B Altered lower vitrophyre	3A Nonwelded vitric tuff	3B Nonwelded zeolitic tuff, alkalic suite	3C Nonwelded zeolitic tuff, calcic suite
Diagenetic zone		I		I		II	II
Sample[2]	67FB-3E	G2-675	25A1-1280	G4-1314	GU3-1498	G4-1544C	25A1-1323
SiO_2	72.9	64.3	74.0	70.2	74.5	69.1	69.1
TiO_2	0.28	0.33	0.10	0.14	0.10	0.06	0.11
Al_2O_3	13.9	16.8	12.4	16.7	11.7	11.5	13.4
Fe_2O_3	1.4	1.83[3]	1.07[3]	1.44[3]	1.10[3]	0.81	1.13[3]
FeO	0.04					0.04	
MnO	0.06	0.17	0.08	0.09	0.08	0.03	0.05
MgO	0.33	1.77	0.31	0.90	0.12	0.03	0.94
CaO	0.92	2.60	0.66	3.51	0.77	0.75	3.22
Na_2O	3.8	1.38	3.40	1.90	3.20	2.82	1.23
K_2O	5.1	2.72	4.00	0.72	4.34	4.10	2.64
P_2O_5	0.02	0.05	0.01	0.02	0.01	0.00	0.01
LOI[4]	0.97	8.0	3.79	5.91	3.58	10.6	8.90
	99.7	100.0	99.8	101.5	99.5	99.8	100.7
Si	68.4	66.0	72.2	69.6	73.0	72.8	71.6
Ti	0.20	0.25	0.07	0.10	0.07	0.04	0.09
Al	15.4	20.3	14.3	19.5	13.5	14.3	16.3
Fe^{3+}	0.98	1.41[3]	0.78[3]	1.07[3]	0.81[3]	0.64	0.88[3]
Fe^{2+}	0.03					0.03	
Mn	0.04	0.12	0.05	0.06	0.05	0.02	0.04
Mg	0.46	2.71	0.45	1.33	0.17	0.05	1.45
Ca	0.93	2.86	0.69	3.73	0.81	0.84	3.58
Na	6.93	2.74	6.43	3.65	6.08	5.76	2.47
K	6.68	3.56	4.98	0.91	5.43	5.51	3.49
P	0.02	0.04	0.01	0.02	0.01	0.00	0.01

Table 7. Continued.

	Prow Pass Member, Crater Flat Tuff			Bullfrog Member, Crater Flat Tuff			Tram Member, Crater Flat Tuff		
	4A Nonwelded vitric tuff	4B Nonwelded zeolitic tuff, alkalic suite	4C Nonwelded zeolitic tuff, calcic suite	5A Partially welded devitrified tuff	5B Nonwelded zeolitic tuff, alkalic suite	5C Nonwelded zeolitic tuff, calcic suite	6A Partially welded devitrified tuff	6B Nonwelded zeolitic tuff, alkalic suite	6C Nonwelded zeolitic tuff, calcic suite
Diagenetic zone		II	II		II	II		II	II
Sample[2]	GU3-1598	GU3-1986B	G4-2131C	J13-2133	G1-2557	25B1H-2879C	J13-2982	G3-3589C	G4-2792B
SiO_2	73.1	67.9	65.7	75.3	69.0	66.9	74.8	66.5	67.9
TiO_2	0.11	0.10	0.12	0.11	0.11	0.26	0.16	0.49	0.15
Al_2O_3	12.2	12.4	13.2	12.6	12.4	13.2	12.2	13.8	12.3
Fe_2O_3	1.41[3]	1.20	1.12	1.44[3]	1.51[3]	1.48	1.41[3]	2.59	1.04
FeO		0.03	0.12			0.24		0.26	0.13
MnO	0.10	0.07	0.02	0.09	0.05	0.04	0.05	0.06	0.03
MgO	0.20	0.11	0.15	0.23	0.22	1.32	0.21	0.57	0.18
CaO	0.83	0.87	2.63	0.75	1.33	3.24	0.89	1.82	2.93
Na_2O	3.29	3.44	2.46	4.02	3.60	1.18	3.70	2.98	2.68
K_2O	4.37	3.72	3.52	4.38	3.05	3.90	4.46	3.65	1.68
P_2O_5	0.02	0.02	0.00	0.03	0.00	0.00	0.02	0.00	0.03
LOI[4]	3.41	10.2	11.1	0.30	7.88	7.86	0.94	7.23	10.9
	99.0	100.1	100.1	99.3	99.1	99.7	98.8	100.0	100.1
Si	71.7	70.7	69.4	71.1	70.8	69.2	71.5	67.4	72.0
Ti	0.08	0.08	0.09	0.08	0.08	0.20	0.11	0.37	0.12
Al	14.1	15.2	16.4	14.0	15.0	16.1	13.8	16.5	15.4
Fe^{3+}	1.04[3]	0.94	0.89	1.02[3]	1.17[3]	1.15	1.01[3]	1.98	0.83
Fe^{2+}		0.03	1.11			0.21		0.22	0.11
Mn	0.07	0.05	0.01	0.06	0.03	0.03	0.03	0.04	0.02
Mg	0.29	0.17	0.24	0.32	0.34	2.03	0.30	0.86	0.28
Ca	0.87	0.97	2.98	0.76	1.46	3.59	0.91	1.98	3.33
Na	6.26	6.94	5.04	7.36	7.16	2.37	6.86	5.86	5.51
K	5.47	4.94	4.75	5.27	3.99	5.15	5.44	4.72	2.27
P	0.02	0.02	0.00	0.02	0.00	0.00	0.02	0.00	0.03

[1] Analyses by combination of X-ray fluorescence, atomic absorption, and plasma emission spectrophotometry.
[2] Analysis of sample 67FB-3E from Quinlivan and Byers (1977) and sample G1-2557 from Zielinski (1983).
[3] Total Fe as Fe_2O_3.
[4] Loss on ignition, determined by difference in sample weight at room temperature and sample weight at 900°C. LOI for G2-675 not measured but determined by difference in analytical total from 100%.

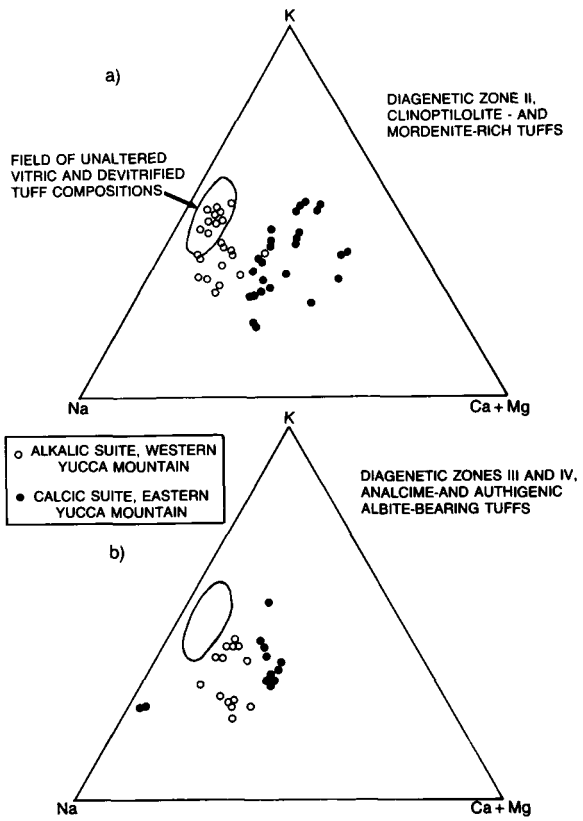

Figure 11. Triangular plots showing alkali and alkaline earth compositions in bulk rock samples, Yucca Mountain, Nevada.

IV represents a further alteration of the zone III assemblage in the deepest part of the volcanic pile, the formation of these deeper diagenetic zones was probably an evolutionary process, the boundaries of zones III and IV rising within the stratigraphic sequence over time. The present-day boundaries of these deeper zones, however, were established at what is probably the time of the most intense diagenetic alteration, which, based on geologic evidence discussed above for zone II, occurred between 11.3 and 13.9 m.y. ago. Authigenic illites from zones III and IV in drill holes USW G-1 and USW G-2 have K-Ar dates of 10.9 ± 0.6 m.y., suggesting that the deeper, more intense alteration was contemporaneous with volcanism associated with Timber Mountain volcanism (Bish, 1986).

Relation of zeolitization to regional water table

At Yucca Mountain, diagenetic zone II straddles the present-day water table; however, the location and role of the water table during zeolitization is uncertain. Hay (1963) and Walton (1975) in studies of the John Day Formation, Oregon, and Vieja Group, Texas, respectively, believed that the alteration of volcanic glass to clinoptilolite occurred in the unsaturated zone as recharge percolated downward through vitric tuffs. Zeolites formed where the percolating recharge became sufficiently alkaline and enriched in total dissolved solids. At Yucca Mountain, the alteration of fine volcanic dust in vitric tuffs and crystallization of smectite in zone I suggest that percolating ground waters leached volcanic glass in the unsaturated zone; however, the nonwelded vitric tuffs available for leaching were relatively thin and varied in thickness (80–165 m). We consider it unlikely that recharge passing downward along complicated flow paths through vitric tuffs of variable thickness would have formed a planar interface at which ground-water compositions became capable of transforming volcanic glass to clinoptilolite.

Hoover (1968) also suggested that the alteration of volcanic glass to zeolites initially occurred in the unsaturated zone. According to Hoover, the position of many zeolite beds above the water table at the NTS is due to local zones of saturation where downward movement of recharge was slowed above impermeable barriers, such as densely welded ash flows, lavas, clay-rich horizons, and pre-existing zeolite beds. Where glass was available, additional zeolites formed in these zones of saturation. Over a long period of time, the zone of saturation was displaced several hundred meters upwards above impermeable barriers by continued thickening of zeolite layers. At Yucca Mountain, the clinoptilolite and heulandite occurrences in zone I may have formed in this manner, but on a relatively small scale. The thick zeolitic tuffs in diagenetic zone II occur as much as 225 m above the water table and may have also formed in this manner. The lack of significant alteration in vitric tuffs within the upper part of the volcanic sequence, except for drill hole USW G-2, however, suggests that zeolitic alteration in zone II was partly a function of depth and related in some way to the water table.

A third explanation for the position of zone II astride the present-day water table (Figure 4) is that the alteration of glass to clinoptilolite in zone II occurred at or below the regional water table and that the zeolitic tuffs were subsequently uplifted by basin-and-range faulting. Stratigraphic units such as the tuff of Calico Hills are thoroughly zeolitic in the structurally low eastern half of Yucca Mountain, but are vitric in the western half, where eastward dips elevate these units high above the present-day water table. The interface between zone I and zone II is tilted in the same direction but to a lesser degree than the tuff of Calico Hills (Figure 3), suggesting that the zeolitic beds were altered before tectonism ended 11.3 m.y. ago.

Factors controlling diagenesis

The distribution, mineralogy, and modes of occurrence of diagenetic minerals at Yucca Mountain are

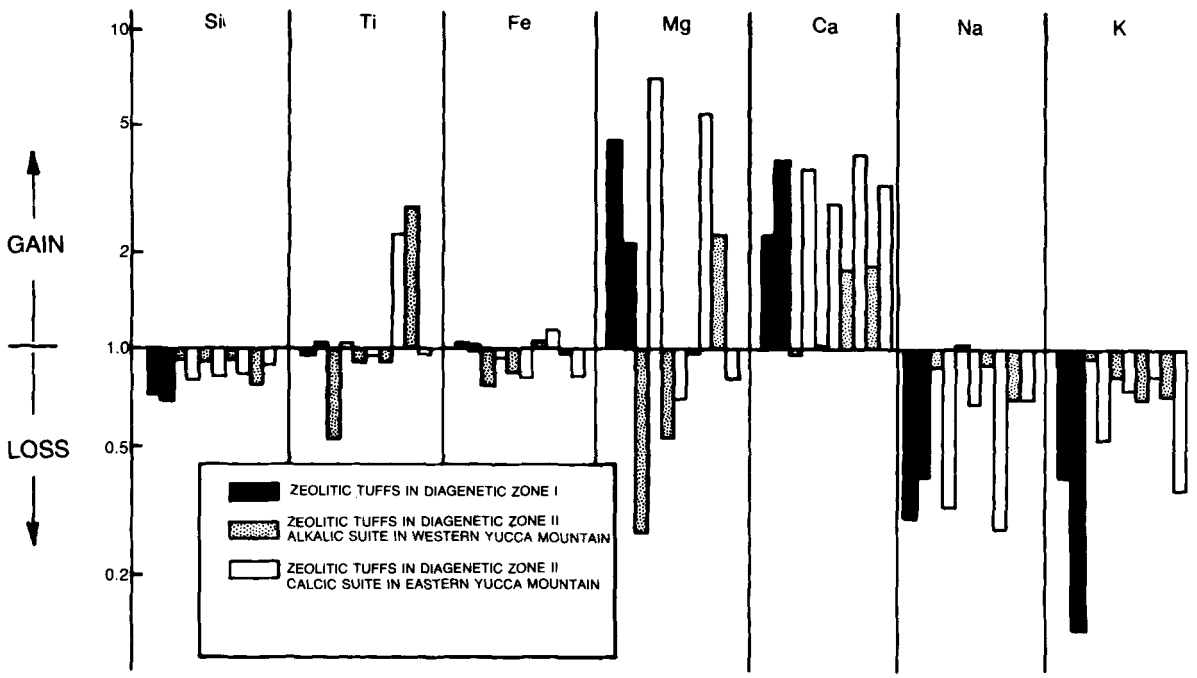

Figure 12. Logarithmic plot showing chemical differences between zeolitic and unaltered tuffs, Yucca Mountain, Nevada. Plot is ratio of element percentage in zeolitic tuff divided by element percentage in unaltered tuff. All compositions are from Table 7 and are normalized to the aluminum concentration of the unaltered tuff.

similar to other occurrences formed in open chemical systems, such as the John Day Formation, Oregon (Hay, 1963); Esmeralda County, Nevada (Robinson, 1966; Moiola, 1970); the Vieja Group, Texas (Walton, 1975); and Desatoya Mountains, Nevada (Barrows, 1980). The chemical and physical processes responsible for the diagenesis of tuffs at Yucca Mountain were probably similar to those at these other occurrences.

Zeolites in diagenetic zone I. The zone I zeolite occurrences on top of the basal vitrophyre of the Topopah Spring Member and of the Yucca Mountain, Pah Canyon, and Upper Topopah Spring Members in drill hole USW G-2 are incompletely understood. Despite their different lithologic settings, both occurrences are above present and paleo-water tables, their zeolites are very calcic despite the Ca-poor nature of the glasses from which they formed, and zeolites are subordinate to smectites. These two occurrences appear to represent locally saturated conditions where descending water slowed by impermeable barriers saturated a tuff containing volcanic glass. Formation of these zeolites was accompanied by the introduction of Ca and Mg and the loss of Si, Na, and K in the rocks (Table 7, samples 1B and 2B; Figure 12). The source of Ca in these rocks is problematic, because the precursor vitric tuffs were Ca-poor (Table 7, samples 1A and 2A).

Levy (1984a, 1984b) concluded that the zeolites on top of the Topopah Spring vitrophyre formed during the late stages of devitrification, during cooling of the ash flow. Based on experimental work by Claassen and White (1979), she suggested that the Ca for these zeolites may have been concentrated in pore waters by the selective leaching of overlying devitrified tuffs.

White *et al.* (1980) showed that recharge-water compositions at Rainier Mesa, located 50 km NNE of Yucca Mountain, became enriched in Na and depleted in Ca and Mg after passing through zeolitic tuffs in the unsaturated zone. They concluded that zeolites and smectites selectively removed bivalent cations from the ground-water system. Similarly, clinoptilolite-group minerals in zone I at Yucca Mountain are Ca-rich because these minerals may have taken up bivalent cations from waters passing downward through the unsaturated zone.

An alternative source of Ca for these zeolites might be zones of caliche developed near the surface. Calcite-filled fractures extending down from these zones show that near-surface carbonates have dissolved in recharge water and then reprecipitated below. If the Ca were derived from caliche, the exchangeable-cation compositions of the zeolites in zone I may have been established more recently than the zones of extensive zeolitization in zone II.

Zeolites in diagenetic zone II. Diagenetic zone II is characterized by nearly complete replacement of glass by clinoptilolite-group minerals. Textural relations

show that clinoptilolite-group minerals crystallized in open cavities left by glass dissolution. Hay (1963, 1966) suggested that glass dissolution creates a favorable environment for zeolite formation by increasing the salinity and pH of pore waters.

At Yucca Mountain, dissolution of high-silica rhyolitic glass probably resulted in pore waters rich in Si and alkalis. The pH of these pore waters may have controlled the species of zeolite formed (Mariner and Surdam, 1970; Donahoe and Dibble, 1982). In general, neutral to moderate pH (7–9) favors the formation of zeolites having high Si/Al ratios. The widespread occurrence of clinoptilolite-group minerals in zone II therefore suggests that pore waters were silica-rich, saline, and slightly basic.

The exchangeable cation compositions of clinoptilolite-group minerals at Yucca Mountain vary systematically both vertically and laterally. These compositions may represent original compositions at the time of their formation or compositions acquired at a later date. The exchangeable cation compositions in clinoptilolite-group minerals may be influenced by original glass compositions, ground-water compositions, and the mineral's cation exchange properties. The composition of the parent vitric tuff apparently was not responsible for the variation in the cation composition of the clinoptilolite-group minerals, because glass compositions are similar throughout the volcanic sequence. Therefore, compositional variations in clinoptilolite-group minerals must be due to differences in the composition of ground waters and/or to the mineral's cation-exchange properties.

For the major constituents of ground water, clinoptilolite has a cation selectivity of K > Ca > Na and Ca > Mg (Ames, 1960; Vaughan, 1978). The effect of cation selectivity is demonstrated by clinoptilolites in deep sea sediments, which uniformly have a K:Na:Ca:Mg ratio of 51:40:4:6, although they are in contact with marine interstitial pore waters having a K:Na:Ca:Mg ratio of 1:85:6:8 (Boles and Wise, 1978). These data show the strong selectivity of clinoptilolite for K in the presence of competing cations.

At Yucca Mountain, clinoptilolite-group minerals are relatively K-rich at the top of zone II. The decrease of K in clinoptilolite with depth (Figure 8) suggests a vertical gradient in ground-water chemistry, with K being selectively removed from ground water by clinoptilolite at the top of zone II. This type of vertical chemical gradient has been described as a percolating open-chemical system by Hay (1963) and Hoover (1968). The K enrichment of clinoptilolite-group minerals in the upper part of zone II may reflect cation exchange between modern recharge water passing through the unsaturated zone and through those portions of zeolitic beds elevated above the water table by tectonism. The trend towards Na-rich clinoptilolite-group minerals with increasing depth in the western part of Yucca Mountain and towards Ca-rich clinoptilolite-group minerals on the east side of Yucca Mountain is more difficult to explain in terms of a percolating ground-water system. Tuffs of similar character and thickness overlie zeolitic rocks throughout Yucca Mountain; hence, significant lateral variations in the chemistry of ground water percolating through the unsaturated zone should not be expected.

The calcic nature of clinoptilolite-group minerals in eastern Yucca Mountain and the alkalic nature of clinoptilolite-group minerals to the west probably reflect ground-water conditions below the water table. Present-day ground-water compositions also become more calcic and less sodic eastward (Benson *et al.,* 1983). Paleozoic limestone and dolomite underlie the tuff aquifers and may have provided a source of Ca in ground water in the eastern part of Yucca Mountain. These carbonates occur at substantially shallower depths beneath eastern Yucca Mountain (Carr *et al.,* 1986). Winograd and Thordarson (1975) divided ground water of the NTS into three major types: (1) Ca-Mg-bicarbonate water in Paleozoic carbonate aquifers, (2) Na-K-bicarbonate water in tuff aquifers, and (3) Ca-Mg-Na-bicarbonate water in areas of cross flow and mixing of the first two types. Most ground waters of Yucca Mountain are Na-K-bicarbonate types typical of tuff aquifers, but an integral water sample from eastern Yucca Mountain in drill hole UE-25p#1 is similar to mixed water of the Ca-Mg-Na-bicarbonate type (Benson *et al.,* 1983; Ogard and Kerrisk, 1984). The trend towards more calcic compositions of clinoptilolite-group minerals with increasing depth in eastern Yucca Mountain may represent progressive dilution of ground water from the tuff aquifer with Ca-Mg-bicarbonate ground water from the Paleozoic carbonate aquifer.

Calcite is more abundant on the eastern side of Yucca Mountain than on the western side. This difference may be due to Ca-rich solutions migrating upwards from the Paleozoic carbonate aquifers, providing a source of abundant Ca. Because calcite occurs only within analcime and albite-bearing tuffs, however, its crystallization may have been controlled by the release of Ca during the transformation of Ca-rich clinoptilolite-group minerals to analcime. If so, the lateral chemical variations at Yucca Mountain predate the formation of vertical mineralogic zones.

Mordenite coexists with clinoptilolite in lower zone II in northern Yucca Mountain. The formation of mordenite is promoted by increased Na and Si contents of reacting solutions or by an increased temperature of crystallization (Höller and Wirsching, 1978; Hawkins *et al.,* 1978). Bulk rock analyses show that mordenite-bearing tuffs are neither more sodic nor more silicic than zeolitic tuffs containing clinoptilolite-group minerals only. Restriction of mordenite to northern Yucca

Mountain therefore is probably due to progressively higher temperatures northward during diagenesis.

Diagenetic minerals in zones III and IV. Analcime and authigenic albite in diagenetic zones III and IV, respectively, are probably due to the transformation of clinoptilolite to progressively less hydrous minerals with increasing temperature at depth. A similar zonation might be expected where ground water became increasingly sodic or less silicic with depth, but bulk-rock chemistry shows that zones III and IV probably formed in an essentially closed chemical system with no Na-enrichment compared to clinoptilolite-bearing rocks in zone II. Kerrisk (1983) concluded that aqueous silica activity decreases from waters in equilibrium with cristobalite to waters in equilibrium with quartz, and controls the mineral evolution with depth. Therefore, the deeper diagenetic zones at Yucca Mountain may be an indirect result of the transformation of cristobalite to quartz with depth.

In northern Yucca Mountain, the boundaries between diagenetic zones are 250–700 m higher and generally thinner than in drill hole USW G-3 to the south, suggesting more intense diagenetic alteration northward. This is especially notable in drill hole USW G-2 in northern Yucca Mountain, which is characterized by marked thinning of zone III, transition from smectite to interstratified illite/smectite at relatively shallow depths, and occurrence of sulfides, barite, and fluorite in zone IV (Caporuscio *et al.,* 1982). These features suggest that the geothermal gradient was progressively greater northward during diagenesis. This hypothesis is supported by a comparison of clay mineralogy in drill holes USW G-3, USW G-1, and USW G-2 (Bish, 1986).

The present-day geothermal gradient at Yucca Mountain ranges from 20° to 40°C/km; the higher gradients are in the northern part of Yucca Mountain (Sass *et al.,* 1983). Based on these gradients, present temperatures at the boundaries of diagenetic zones are 32°–41°C between zones II and III and 41°–55°C between zones III and IV. These deeper diagenetic zones probably did not form under the present temperature conditions. Ground water would have had to be saline brines containing 10^5 ppm Na^+ to form analcime and authigenic albite at such low temperatures (Iijima, 1975; Smyth and Caporuscio, 1981). No evidence exists for subsurface brines in the NTS region (Winograd and Thordarson, 1975), and modern ground water tested at Yucca Mountain generally contains <100 ppm Na^+ (Benson *et al.,* 1983).

Thus, the present diagenetic zone boundaries at Yucca Mountain were established during an earlier period of higher geothermal gradient probably associated with emplacement of upper crustal magma chambers of the Timber Mountain-Oasis Valley caldera complex to the north. The regional geothermal gradient probably reached a maximum during culminating ash-flow eruptions of the Paintbrush and Timber Mountain Tuffs between 11.1 and 13.3 m.y. ago (Byers *et al.,* 1976; Marvin *et al.,* 1970). The upward displacement and thinning of diagenetic zones northward is likely due to a higher geothermal gradient in northern Yucca Mountain which was closer to the locus of silicic volcanism.

SUMMARY AND CONCLUSIONS

Rhyolitic ash-flow tuffs at Yucca Mountain, Nevada, host vertically and laterally extensive diagenetic mineral deposits. Diagenetic alteration was largely controlled by lithology, with most deposits occurring within nonwelded ash-flow tuffs and in nonwelded tops and bottoms of ash flows that have moderately to densely welded, devitrified interiors. These nonwelded tuffs remained vitric and permeable after emplacement and were highly susceptible to alteration by ground water. The diagenetic mineral assemblages formed in these tuffs are vertically zoned, becoming progressively less hydrous with depth. The development of vertically zoned mineral assemblages was probably an evolutionary process in which clinoptilolite-bearing tuffs were replaced by analcime at intermediate depths, and analcime was replaced by authigenic albite in the deepest parts of the volcanic pile.

The mineralogy and chemistry of zeolitic tuffs at Yucca Mountain are similar to other zeolite occurrences in silicic volcanic and volcaniclastic rocks. Alteration of volcanic glass to clinoptilolite-group minerals occurred in an open chemical system, resulting in significant rearrangement of mobile cations in the host tuffs. Chemical changes were most pronounced in eastern Yucca Mountain, where Ca-rich tuffs developed. Chemical alteration was less significant in western Yucca Mountain, where the altered tuffs are generally more alkalic.

The analcime- and albite-bearing tuffs are chemically zoned laterally, similar to tuffs containing clinoptilolite-group minerals. Thus, the transformation from clinoptilolite to analcime- and authigenic albite-bearing rocks occurred under conditions in which chemical migration was restricted, probably because of the low permeability of the zeolitic tuffs during the mineralogic transformations.

Lateral chemical variations within the diagenetically altered tuffs probably occurred during the initial stages of alteration of glass to clinoptilolite-group minerals, but may also reflect some exchange with modern ground waters. Ca- and Mg-enrichment of zeolitic tuffs in eastern Yucca Mountain probably reflects ion exchange between clinoptilolite-group minerals and calcic ground waters derived in part from Paleozoic carbonates underlying these tuffs.

Vertically zoned diagenetic mineral assemblages

formed in response to mineralogic transformations to more stable minerals as temperatures rose during progressive burial of the tuffs. Diagenetic zones also rise in elevation and thin northward, reflecting higher temperatures in that direction. The present diagenetic zone boundaries did not form in response to the modern geothermal gradient, but instead developed in response to a thermal pulse caused by the emplacement of high-level crustal magma chambers within the Timber Mountain-Oasis Valley caldera complex to the north.

ACKNOWLEDGMENTS

We thank Roland Hagan and Gary Luedemann for analysis of the bulk-rock samples by XRF and David Mann for preparation of polished thin sections. Marcia Jones typed the manuscript, and Anthony Garcia and Florence Fujita prepared the illustrations. We also thank J. R. Boles, R. L. Hay, F. A. Mumpton, R. A. Sheppard, and D. T. Vaniman for critical reviews of the manuscript.

This work was supported by the Nevada Nuclear Waste Storage Investigations (NNWSI) Project as part of the Civilian Radioactive Waste Management Program. The NNWSI Project is managed by the Waste Management Project Office of the DOE Nevada Operations Office. NNWSI project work is sponsored by the Office of Geologic Repositories of the DOE Office of Civilian Radioactive Waste Management.

REFERENCES

Ames, L. L., Jr. (1960) The cation sieve properties of clinoptilolite: *Amer. Mineral.* **45,** 689–700.

Arney Carlos, B. (1985) Minerals in fractures of the unsaturated zone from drill core USW G-4, Yucca Mountain, Nye County, Nevada: *Los Alamos Nat. Lab. Rept.* **LA-10415-MS,** 55 pp.

Barrows, K. J. (1980) Zeolitization of Miocene volcaniclastic rocks, southern Desatoya Mountains, Nevada: *Geol. Soc. Amer. Bull.* **91,** 199–210.

Bence, A. E. and Albee, A. L. (1968) Empirical correction factors for electron microanalysis of silicates and oxides: *J. Geol.* **76,** 382–403.

Benson, L. V., Robinson, J. H., Blankennagel, R. K., and Ogard, A. E. (1983) Chemical composition of groundwater and the locations of permeable zones in the Yucca Mountain area, Nevada: *U.S. Geol. Surv. Open-File Rept.* **83-854,** 19 pp.

Bish, D. L. (1986) Evaluation of past and future alterations in tuff at Yucca Mountain, Nevada, based on the clay mineralogy of drill cores USW G-1, G-2, and G-3: *Los Alamos Nat. Lab. Rept.* **LA-10667-MS,** 42 pp.

Bish, D. L., Caporuscio, F. A., Copp, J. F., Crowe, B. M., Purson, J. D., Smyth, J. R., and Warren, R. G. (1981) Preliminary stratigraphic and petrologic characterization of core samples from USW G-1, Yucca Mountain, Nevada: *Los Alamos Nat. Lab. Rept.* **LA-8840-MS,** 66 pp.

Bish, D. L. and Semarge, E. (1982) Mineralogic variations in a silicic tuff sequence: Evidence for diagenetic and hydrothermal reactions: *Prog. Abstracts, 19th Annual Meeting, Clay Minerals Soc., Hilo, Hawaii,* **42,** (abstract).

Bish, D. L. and Vaniman, D. T. (1985) Mineralogic summary of Yucca Mountain, Nevada: *Los Alamos Nat. Lab. Rept.* **LA-10543-MS,** 55 pp.

Boles, J. R. (1971) Synthesis of analcime from natural heulandite and clinoptilolite: *Amer. Mineral.* **56,** 1724–1734.

Boles, J. R. (1972) Composition, optical properties, cell dimensions, and thermal stability of some heulandite group zeolites: *Amer. Mineral.* **57,** 1463–1493.

Boles, J. R. and Wise, W. S. (1978) Nature and origin of deep-sea clinoptilolite: in *Natural Zeolites: Occurrence, Properties, Use,* L. B. Sand and F. A. Mumpton, eds., Pergamon Press, Elmsford, New York, 235–243.

Broxton, D. E., Vaniman, D. T., Caporuscio, F., Arney, B., and Heiken, G. (1982) Detailed petrographic and microprobe data for drill holes USW G-2 and UE25b-1H, Yucca Mountain, Nevada: *Los Alamos Nat. Lab. Rept.* **LA-9324-MS,** 168 pp.

Broxton, D. E., Warren, R. G., Hagan, R. C., and Luedemann, G. (1986) Chemistry of diagenetically-altered tuffs at a potential nuclear waste repository, Yucca Mountain, Nye County, Nevada: *Los Alamos Nat. Lab. Rept.* **LA-10802-MS,** 160 pp.

Byers, F. M., Jr., Carr, W. J., Orkild, P. P., Quinlivan, W. D., and Sargent, K. A. (1976) Volcanic suites and related cauldrons of Timber Mountain-Oasis Valley caldera complex, southern Nevada: *U.S. Geol. Surv. Prof. Pap.* **919,** 70 pp.

Caporuscio, F., Vaniman, D., Bish, D., Broxton, D., Arney, B., Heiken, G., Byers, F., Gooley, R., and Semarge, E. (1982) Petrologic studies of drill cores USW G-2 and UE25b-1H, Yucca Mountain, Nevada: *Los Alamos Nat. Lab. Rept.* **LA-9255-MS,** 111 pp.

Carr, W. J. (1984) Regional structural setting of Yucca Mountain, southwestern Nevada, and late Cenozoic rates of tectonic activity in part of the southwestern Great Basin, Nevada and California: *U.S. Geol. Surv. Open-File Rept.* **84-354,** 109 pp.

Carr, W. J., Byers, F. M., Jr., and Orkild, P. P. (1984) Stratigraphic and volcano-tectonic relations of Crater Flat Tuff and some older volcanic units, Nye County, Nevada: *U.S. Geol. Surv. Open-File Report* **84-114,** 42 pp.

Carr, M. D., Waddell, S. J., Vick, G. S., Stock, J. M., Monsen, S. A., Harris, A. G., Cork, B. S., and Byers, F. M., Jr. (1986) Geology of drill-hole UE25p#1: A test hole to pre-Tertiary rocks near the potential nuclear waste disposal site at Yucca Mountain, southern Nevada: *U.S. Geol. Surv. Open-File Rept.* **86-175,** 88 pp.

Christiansen, R. L., Lipman, P. W., Carr, W. J., Byers, F. M., Jr., Orkild, P. P., and Sargent, K. A. (1977) Timber Mountain-Oasis Valley caldera complex of southern Nevada: *Geol. Soc. Amer. Bull.* **88,** 943–959.

Christiansen, R. L., Lipman, P. W., Orkild, P. P., and Byers, F. M., Jr. (1965) Structure of the Timber Mountain caldera, southern Nevada, and its relation to basin-range structure, in *U.S. Geol. Surv. Prof. Pap.* **525B,** B43–B48.

Claassen, H. C. and White, A. F. (1979) Application of geochemical kinetic data to groundwater systems: A tuffaceous-rock system in southern Nevada: *Amer. Chem. Soc. Symp. Ser.* **93,** 771–793.

Coombs, D. S. and Whetten, J. T. (1967) Composition of analcime from sedimentary and burial metamorphic rocks: *Geol. Soc. Amer. Bull.* **78,** 269–282.

Criss, J. (1980) Fundamental parameters calculations on a laboratory microcomputer: *Adv. X-Ray Analysis* **23,** 93–97.

Donahoe, R. J. and Dibble, W. E. (1982) Some observations on the mechanism of zeolite crystallization: *Geol. Soc. Amer. Abs. with Prog.* **14,** p. 476.

Hawkins, D. B., Sheppard, R. A., and Gude, A. J., 3rd (1978) Hydrothermal synthesis of clinoptilolite and comments on the assemblage phillipsite-clinoptilolite-mordenite: in *Natural Zeolites: Occurrence, Properties, Use,* L. B. Sand and F. A. Mumpton, eds., Pergamon Press, Elmsford, New York, 337–343.

Hay, R. L. (1963) Stratigraphy and zeolite diagenesis of the John Day Formation of Oregon: *Univ. Calif. Publ. Geol. Sci.* **42,** 199–262.

Hay, R. L. (1966) Zeolites and zeolitic reactions in sedimentary rocks: *Geol. Soc. Amer. Spec. Pap.* **85,** 130 pp.

Heiken, G. H. and Bevier, M. L. (1979) Petrology of tuff units from the J-13 drill site, Jackass Flats, Nevada: *Los Alamos Nat. Lab. Rept.* **LA-7563-MS,** 55 pp.

Höller, H. and Wirsching, U. (1978) Experiments on the formation of zeolites by hydrothermal alteration of volcanic glass: in *Natural Zeolites: Occurrence, Properties, Use,* L. B. Sand and F. A. Mumpton, eds., Pergamon Press, Elmsford, New York, 175–198.

Hoover, D. L. (1968) Genesis of zeolites, Nevada Test Site: *Geol. Soc. Amer. Mem.* **100,** 275–284.

Iijima, A. (1975) Effect of pore water to clinoptilolite-analcime-albite reaction series: *J. Fac. Sci., Univ. Tokyo, Sec. II* **19,** 133–147.

Iijima, A. (1978) Geologic occurrences of zeolites in marine environments: in *Natural Zeolites: Occurrence, Properties, Use,* L. B. Sand and F. A. Mumpton, eds., Pergamon Press, Elmsford, New York, 175–198.

Iijima, A. (1980) Geology of natural zeolites and zeolitic rocks: in *Proc. 5th Int. Conf. Zeolites, Naples, 1980,* L. V. C. Rees, ed., Heyden, London, 103–118.

Johnstone, J. K. and Wolfsberg, K., eds. (1980) Evaluation of tuff as a medium for a nuclear waste repository: Interim status report on the properties of tuff: *Sandia Nat. Lab. Rept. SAND80-1464,* 134 pp.

Kastner, M. and Siever, R. (1979) Low temperature feldspars in sedimentary rocks: *Amer. J. Sci.* **279,** 435–479.

Kerrisk, J. F. (1983) Reaction path calculations of groundwater chemistry and mineral formation at Rainier Mesa, Nevada: *Los Alamos Nat. Lab. Rept.* **LA-9912-MS,** 41 pp.

Kirov, G. N., Pechigargov, V., and Landzheve, E. (1979) Experimental crystallization of volcanic glasses in a thermal gradient field: *Chem. Geol.* **26,** 17–28.

Levy, S. S. (1984a) Petrology of samples from drill holes USW H-3, H-4, and H-5, Yucca Mountain, Nevada: *Los Alamos Nat. Lab. Rept.* **LA-9706-MS,** 77 pp.

Levy, S. S. (1984b) Studies of altered vitrophyre for the prediction of nuclear waste repository-induced thermal alteration at Yucca Mountain, Nevada: in *Scientific Basis for Nuclear Waste Management, Proc. 7th Material Research Soc. Symposia,* G. L. McVay, ed., Elsevier, New York, 959–966.

Lipman, P. W. (1965) Chemical comparison of glassy and crystalline volcanic rocks: *U.S. Geol. Surv. Bull.* **1201-D,** 24 pp.

Lipman, P. W., Christiansen, R. L., and O'Conner, J. T. (1966) A compositionally zoned ash-flow sheet in southern Nevada: *U.S. Geol. Surv. Prof. Pap.* **524-F,** F1–F47.

Maldonado, F. and Koether, S. L. (1983) Stratigraphy, structure and some petrographic features of Tertiary volcanic rocks at the USW G-2 drill hole, Yucca Mountain, Nye County, Nevada: *U.S. Geol. Surv. Open-File Rept.* **83-732,** 83 pp.

Mariner, R. H. and Surdam, R. C. (1970) Alkalinity and formation of zeolites in saline-alkaline lakes: *Science* **170,** 977–980.

Marvin, R. F., Byers, F. M., Jr., Mehnert, H. H., Orkild, P. P., and Stern, T. W. (1970) Radiometric ages and stratigraphic sequence of volcanic and plutonic rocks, southern Nye and western Lincoln Counties, Nevada: *Geol. Soc. Amer. Bull.* **81,** 2657–2676.

Mason, B. and Sand, L. B. (1960) Clinoptilolite from Patagonia—the relationship between clinoptilolite and heulandite: *Amer. Mineral.* **45,** 341–350.

Moiola, R. J. (1970) Authigenic zeolites and K-feldspars in the Esmeralda Formation, Nevada: *Amer. Mineral.* **55,** 1681–1691.

Moncure, G. K., Surdam, R. C., McKague, H. L. (1981) Zeolite diagenesis below Pahute Mesa, Nevada Test Site: *Clays & Clay Minerals* **29,** 385–396.

Mumpton, F. A. (1960) Clinoptilolite redefined: *Amer. Mineral.* **45,** 351–369.

Nielson, C. H. and Sigurdsson, H. (1981) Quantitative methods for electron microprobe analysis of sodium in natural and synthetic glasses: *Amer. Mineral.* **66,** 547–552.

Noble, D. C. (1967) Sodium, potassium, and ferrous iron contents of some secondarily hydrated natural silicic glasses: *Amer. Mineral.* **52,** 280–286.

Ogard, A. E. and Kerrisk, J. F. (1984) Groundwater chemistry along flow paths between a proposed repository site and the accessible environment: *Los Alamos Nat. Lab. Rept.* **LA-10188-MS,** 48 pp.

Quinlivan, W. D. and Byers, F. M., Jr. (1977) Chemical data and variation diagrams of igneous rocks from the Timber Mountain-Oasis Valley caldera complex, southern Nevada: *U.S. Geol. Surv. Open-File Rept.* **77-724,** 9 pp.

Robinson, P. T. (1966) Zeolitic diagenesis of Mio-Pliocene rocks of the Silver Peak Range, Esmeralda County, Nevada: *J. Sed. Pet.* **36,** 1007–1015.

Sass, J., Lachenbruch, A., Grubb, F., and Moses, T. (1983) Status of thermal observations at Yucca Mountain, Nevada: *U.S. Geol. Surv. Letter Rept.* 10 pp.

Scott, R. B. and Bonk, J. (1984) Preliminary map of Yucca Mountain, Nye County, Nevada, with geologic sections: *U.S. Geol. Surv. Open-File Rept.* **84-494,** scale 1:12000.

Scott, R. B. and Spengler, R. W. (1982) Structural framework of a potential nuclear waste repository, Yucca Mountain, Nevada Test Site: *Amer. Geophys. Union Trans.* **63,** p. 1099.

Scott, R. and Castellanos, M. (1984) Preliminary report on the geologic character of drill holes USW GU-3 and USW G-3: *U.S. Geol. Surv. Open-File Rept.* **84-491,** 121 pp.

Sheppard, R. A. and Gude, A. J., 3rd (1969) Diagenesis of tuffs in the Barstow Formation, Mud Hills, San Bernardino County, California: *U.S. Geol. Surv. Prof. Pap.* **634,** 34 pp.

Sheppard, R. A. and Gude, A. J., 3rd (1973) Zeolites and associated authigenic silicate minerals in tuffaceous rocks of the Big Sandy Formation, Mohave County, Arizona: *U.S. Geol. Surv. Prof. Pap.* **830,** 36 pp.

Sheppard, R. A. and Gude, A. J., 3rd (1985) Diagenetic reaction of clinoptilolite to form mordenite in silicic vitric tuff from Yucca Mountain, Nye County, Nevada, U.S.A.: in *Prog. and Abst., Zeolite '85, Int. Conf. Occurrence, Properties, Utilization of Natural Zeolites, Budapest, 1985,* 17–18 (abstract).

Smyth, J. R. and Caporuscio, F. A. (1981) Review of the thermal stability and cation exchange properties of the zeolite minerals clinoptilolite, mordenite, and analcime: Applications to radioactive waste isolation in silicic tuffs: *Los Alamos Nat. Lab. Rept.* **LA-8841-MS,** 30 pp.

Spengler, R. W., Byers, F. M., Jr., and Warner, J. B. (1981) Stratigraphy and structure of volcanic rocks in drill hole USW-G1, Yucca Mountain, Nye County, Nevada: *U.S. Geol. Surv. Open-File Rept.* **81-1349,** 50 pp.

Spengler, R. W., Muller, D. C., and Livermore, R. B. (1979) Preliminary report on the geology and geophysics of drill

hole UE25a-1, Yucca Mountain, Nevada: *U.S. Geol. Surv. Open-File Rept.* **79-1244,** 43 pp.

Sykes, M. L., Heiken, G. H., and Smyth, J. R. (1979) Mineralogy and petrology of tuff units from the UE25a-1 drill site, Yucca Mountain, Nevada: *Los Alamos Nat. Lab. Rept.* **LA-8139-MS,** 76 pp.

Vaniman, D., Bish, D., Broxton, D., Byers, F., Heiken, G., Carlos, B., Semarge, E., Caporuscio, F., and Gooley, R. (1984) Variations in authigenic mineralogy and sorptive zeolite abundance at Yucca Mountain, Nevada, based on studies of drill cores USW GU-3 and G-3: *Los Alamos Nat. Lab. Rept.* **LA-9707-MA,** 71 pp.

Vaughan, D. E. W. (1978) Properties of natural zeolites: in *Natural Zeolites: Occurrences, Properties, Use,* L. B. Sand and F. A. Mumpton, eds., Pergamon Press, Elmsford, New York, 353–371.

Walton, A. W. (1975) Zeolitic diagenesis in Oligocene volcanic sediments, Trans-Pecos, Texas: *Geol. Soc. Amer. Bull.* **86,** 615–624.

White, A. F., Claassen, H. C., and Benson, L. V. (1980) The effect of dissolution of volcanic glass on the water chemistry in a tuffaceous aquifer, Rainier Mesa, Nevada: *U.S. Geol. Surv. Water-Supply Pap.* **1535-Q,** 34 pp.

Winograd, I. J. and Thordarson, W. (1975) Hydrogeologic and hydrochemical framework, south-central Great Basin, Nevada-California, with special reference to the Nevada Test Site: *U.S. Geol. Surv. Prof. Pap.* **712-C,** 126 pp.

Wirsching, U. (1976) Experiments on hydrothermal alteration processes of rhyolitic glass in closed and open systems: *N. Jb. Miner. Mh.* **5,** 202–213.

Zielinski, R. A. (1983) Evaluation of ash-flow tuffs as hosts for radioactive waste: Criteria based on selective leaching of manganese oxides: *U.S. Geol. Surv. Open-File Rept.* **83-480,** 21 pp.

(Received 13 January 1986; accepted 4 September 1986; Ms. 1551)